CHARACTERIZATION OF OZONE CONTACTOR THROUGH MATHEMATICAL SIMULATION AND DEMONSTRATION OF THE DESTRUCTION OF FREE AND COMPLEXED CYANIDE BY OZONATION

A Thesis Submitted

in Partial Fulfillment of the Requirements

for the Degree of

MASTER OF TECHNOLOGY

in

Environmental Engineering and Management

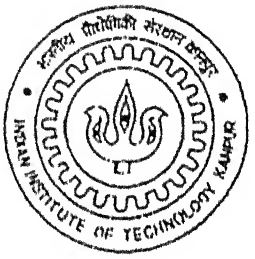

by

RAMAN KUMAR

to the

DEPARTMENT OF CIVIL ENGINEERING

Indian Institute of Technology, Kanpur

June, 2002

3 FEB 2003/CE
पुरूषोत्तम काशीनाथ केलकर पुस्तकालय
भारतीय प्रौद्योगिकी संस्थान कानपुर
अवाप्ति क्र० A 141824

Dedicated to
my dearest
Motherey

CERTIFICATE

It is certified that the work contained in the thesis entitled "***Characterization of Ozone Contactor through Mathematical Simulation and Demonstration of the Destruction of Free and Complexed Cyanide by Ozonation*** ", by Mr. Raman Kumar , has been carried out under my supervision and that this work has not been submitted elsewhere for a degree.

Dr. Purnendu Bose

Assistant Professor

Department of Civil Engineering

Indian Institute of Technology

Kanpur, India

ACKNOWLEDGMENT

Tinku, Motherey, Fatherey and Thakur ji have been always with me to enlighten my path bearing every hurdle of my life. It would have been impossible to reach here without them.

I am deeply indebted to my supervisor Dr. Purnendu Bose for his immense support during my thesis. He advised and assisted me as well in real life problems as in technical and conceptual ones. I can never forget his supporting hand during those 'unemployed days' when I was totally shattered. His act of presenting things and doing work is really unique and marvelous, which I have always tried to follow up. We shared excitement and frustrations encountered in the calculations and in the attempts to interpret them. I will miss him.

My special regards to Dr.Vinod Tare who always kept pumping me to do hard work. I appreciate his approach of dealing things not only in professional life but in daily life also. I always tie-up his lessons taught which were extract of his life time experience. Some life time moments which we shared during Swajal Project are unforgettable to me. I have always appreciated his innovative and creative ideas which he has developed due to intensive hard work from which one should be always inspired of.

Words of thanks to Dr. Binayak Rath, Dr. Malay Chaudhuri and Dr. D.K. Ghosh for their help during my course work. Special thanks to Dr. Saumyen Guha for my favorite course "Fate and Transport of contaminants in natural systems". That was the best paper which I had ever took during course work and got the poorest grade. I express my gratitude to Dr. Mukesh Sharma also.

Above in all it were Mr.S.N.Mishra and Mr.Vijay Singh Yadav who made it possible for me to set up model of project inspite of lot of hurdles. So special thanks to them and Mr. R.B.Lal also who have been always cooperative to me in issuing things (specially Cyanide)

In addition to the aforementioned, I render special thanks to Mr. S.P. Shukla and Mr. P.S. Satwat for their technical advise and friendly support. We shared each and every moment in lab including Triple Distill Water and IC.

When one side of IIT was full of pressure and tensions, other side was joyful because of seniors, friends and juniors.

By heart cooperation of N'nshwars (Jha & Kunz sir), Souvik, Umas & Rakesh sir setted up example before me that how to help juniors.

Dhiman, Chintu, Sandeep and our sabzi Maggie were always there with me. We shared tension, frustration and of course best moments at IIT. That was very nice time with Batedi (Jeetu), Pawan, Suresh, Adwani, Bhakti, Shubham, Shweta, Neha, Amlan, Aaka, Shivali, Sharmaji, Don sahab, Rajnish and one in all our Susham Bhaaaii.

Special love and support I got from Civil engineering guys, Imran Sahab, Santosh, Pankaj, Avinash, Desai. They all were always cooperative to me.

It was totally joyful to interact with my junior batch specially Veee, Manoj, Uday Bhan, Gunjant, Yash, (Telnet) Bhaskar ji, Lavania, Kamlesh, Mayank, Ayan (Bong Effect) , Sinha Ji, Raja, Sanjana, Neeru (Shakuntla) and Shaily. Also enjoyed the Guftgoo with Benzamin sisters- Bhawana and Vishikha (made for each other).

They were Harishankar ji, Sheetal, Sudhir, Dilip Bhai, Jha ji, Vinay, KD bhai and Rinks (Compu expert) who have been helping hands for me during experiments.

Last but not least it was our EEM lab where I spend more time than my room. Apart from doing work I always felt like member of some family and this time I am feeling nostalgic leaving IIT Kanpur, our lab and specially my Guide.

TABLE OF CONTENTS

LIST OF TABLES

LIST OF FIGURES

NOMENCLATURE

Symbol	Description	Units
$P_{[O_3]}$	Partial Pressure of Ozone	atmospheres
$H_{[O_3]}$	Henry's Constant for Ozone	atmospheres
$X_{[O_3]}$	Saturation Mole Fraction of Ozone Corresponding to $[O_3]_g$	$mole.mole^{-1}$
$[O_3]_l^s$	Saturated Aqueous Phase Ozone Concentration Corresponding to $[O_3]_g$	$mg.L^{-1}$
$[O_3]_g$	Gas Phase ozone concentration Inside the Reactor and Effluent from the Reactor	$mg.L^{-1}$
k_1'	Forward Kinetic Rate Constant for Equation 4.3	s^{-1}
k_2'	Backward Kinetic Rate Constant for Equation 4.3	s^{-1}
D_{O_3}	Diffusion Constant of Ozone	$m^2.s^{-1}$
μ	Dynamic viscosity of Water	$N.s.m^{-2}$
k_1	Kinetic Rate Constant for Equation 1 in Table 4.6	$M^{-1}s^{-1}$
k_2	Kinetic Rate Constant for Equation 2 in Table 4.6	$M^{-1}s^{-1}$
k_3	Kinetic Rate Constant for Equation 3 in Table 4.6	$M^{-1}s^{-1}$
k_4	Kinetic Rate Constant for Equation 4 in Table 4.6	$M^{-1}s^{-1}$
k_5	Kinetic Rate Constant for Equation 5 in Table 4.6	s^{-1}
k_6	Kinetic Rate Constant for Equation 6 in Table 4.6	$M^{-1}s^{-1}$
k_7	Kinetic Rate Constant for Equation 7 in Table 4.6	$M^{-1}s^{-1}$
k_8	Kinetic Rate Constant for Equation 8 in Table 4.6	$M^{-1}s^{-1}$
k_9	Kinetic Rate Constant for Equation 9 in Table 4.6	$M^{-1}s^{-1}$
k_{10}	Kinetic Rate Constant for Equation 10 in Table 4.6	$M^{-1}s^{-1}$
k_{11}	Kinetic Rate Constant for Equation 11 in Table 4.6	$M^{-1}s^{-1}$

Symbol	Description	Units
k_{17}	Kinetic Rate Constant for Equation 17 in Table 4.6	$M^{-1}s^{-1}$
k_{19}	Kinetic Rate Constant for Equation 19 in Table 4.6	$M^{-1}s^{-1}$
k_{18}	Kinetic Rate Constant for Equation 18 in Table 4.6	$M^{-1}s^{-1}$
$[OH^-]$	Hydroxide Ion Concentration	M
k_{12}^f	Forward Kinetic Rate Constant for Equation 12 in Table 4.6	s^{-1}
k_{13}^f	Forward Kinetic Rate Constant for Equation 13 in Table 4.6	s^{-1}
k_{14}^f	Forward Kinetic Rate Constant for Equation 14 in Table 4.6	s^{-1}
k_{15}^f	Forward Kinetic Rate Constant for Equation 15 in Table 4.6	s^{-1}
k_{16}^f	Forward Kinetic Rate Constant for Equation 16 in Table 4.6	s^{-1}
k_{12}^b	Backward Kinetic Rate Constant for Equation 12 in Table 4.6	$M^{-1}s^{-1}$
k_{13}^b	Backward Kinetic Rate Constant for Equation 13 in Table 4.6	$M^{-1}s^{-1}$
k_{14}^b	Backward Kinetic Rate Constant for Equation 14 in Table 4.6	$M^{-1}s^{-1}$
k_{15}^b	Backward Kinetic Rate Constant for Equation 15 in Table 4.6	$M^{-1}s^{-1}$
k_{16}^b	Backward Kinetic Rate Constant for Equation 16 in Table 4.6	$M^{-1}s^{-1}$
K_{CN^-,O_3}	Kinetic Rate Constant of Reaction Between Cyanide and Ozone	$M^{-1}s^{-1}$
$K_{CN^-,\bullet OH}$	Kinetic Rate Constant of Reaction Between Cyanide and Hydroxyl Radical	$M^{-1}s^{-1}$
$f_{CN^-,\bullet OH}$	Fraction of Generated Hydroxyl Radicals Reacting with Cyanide (CN^-)	--
$k_{bi,\bullet OH}$	Reaction Rate Constant for the i^{th} By-Product of Cyanide Decomposition with Hydroxyl Radical	$M^{-1}s^{-1}$
M_{bi}	Molar Concentration of the i^{th} By-Product of Cyanide Decomposition	M
$k_{si,\bullet OH}$	Reaction Rate Constant for the i^{th} Solute (Other than those Specifically Accounted for) Present in Water with Hydroxyl Radical	$M^{-1}s^{-1}$

Symbol	Description	Units
M_{si}	Molar Concentration for the i^{th} Solute (Other than those Specifically Accounted for) Present in Water	M
$[CN^-]_i$	Influent Cyanide Concentration	$mg.L^{-1}$
$[O_3]_g^i$	Influent Gaseous Ozone Concentration	$mg.L^{-1}$
$[\bullet O_2^-]$	Super-Oxide Radical Concentration	M
$[\bullet HO_2]$	Hydro-Peroxide Radical Concentration	M
$[HO_2^-]$	Hydro-Peroxyl Ion Concentration	M
$[\bullet O_3^-]$	Ozonide Radical Concentration	M
$[\bullet HO_3]$	Hydrated Ozonide Radical Concentration	M
$[\bullet OH]$	Hydroxyl Radical Concentration	M
$[H_2O_2]$	Hydrogen Peroxide Concentration	M
$[H^+]$	Hydrogen Ion Concentration	M
$[H_2CO_3^*]$	Carbonic Acid Concentration	M
$[HCO_3^-]$	Bicarbonate Ion Concentration	M
$[CO_3^{--}]$	Carbonate Ion Concentration	M
$[\bullet CO_3^-]$	Carbonate Radical Concentration	M
$[O_3]_l$	Aqueous Phase Ozone Concentration Inside and Effluent from the Reactor	$mg.L^{-1}$
$[CN^-]$	Cyanide Ion Concentration Inside the Reactor and Effluent from the Reactor	$mg.L^{-1}$
a	Specific Bubble Surface Area	m^2m^{-3}
A	Column Cross-Section Area	m^2
C_T	Inorganic Carbon Concentration	mM

Symbol	Description	Units
d	Gas Bubble Diameter	mm
K_{12}	Equilibrium Constant for Equation 12 in Table 4.6	M
K_{13}	Equilibrium Constant for Equation 13 in Table 4.6	M
K_{14}	Equilibrium Constant for Equation 14 in Table 4.6	M
K_{15}	Equilibrium Constant for Equation 15 in Table 4.6	M
K_{16}	Equilibrium Constant for Equation 16 in Table 4.6	M
K_L	Specific Transfer Coefficient	$m.s^{-1}$
$K_L.a$	Mass Transfer Coefficient	s^{-1}
N	Number of Bubbles per m^3 of Gas	--
Q_g	Gas Flow Rate	$L.min^{-1}$
Q_l	Liquid Flow Rate	$mL.min^{-1}$
S	Solubility Ratio	$M.M^{-1}$
s	Individual Bubble Surface Area	m^2
T	Temperature	^oC
U	Superficial Gas Velocity	$m.s^{-1}$
v	Individual Bubble Volume	m^3
V	Volume of Reactor	L

ABSTRACT

The objective of the research described in this dissertation was twofold. First, mechanistic modeling of continuous flow counter current ozone contactor, followed by experimental verification of model simulation results. Second, conducting experimental studies under various physical and chemical conditions for the determination of the rate and extent of degradation of free and copper-complexed cyanide by ozonation, and monitoring the consequent evolution of ozonation by-products. As per the first objective, a continuous flow counter-current ozone contactor was modeled by incorporating concepts describing rate and extent of ozone mass transfer from gaseous to aqueous phases, and comprehensive consideration of ozone decomposition reactions in the aqueous phase. Experimental verification of model simulation results concerning aqueous ozone concentration in the reactor, and effluent gaseous ozone concentration from the reactor showed only modest correlation between the experimental and simulated results. Discrepancy between some experimental and simulation results were attributed to difference in temperature and ionic strength between the experimental and simulation conditions. As per the second objective, high pH aqueous solutions of free and copper-complexed cyanide were treated by ozonation in continuous flow counter-current ozone contactors at various liquid throughput rates and scavenger concentration. Results indicated that greater than 90 percent removal of free cyanide may be obtained with an influent gaseous ozone concentration of 40 mg/L, liquid throughput of 25 mL/min and scavenger concentration (C_T) of 1, 2 or 3 mM. Ozone requirement for achieving such decomposition varies between 6.45 moles (C_T = 3 mM) to 7.29 moles (C_T = 1 mM) of ozone per mole of cyanide destroyed. At higher and lower values of liquid throughput i.e., 30 mL/min and 10 mL/min respectively and C_T = 3 mM, cyanide removal percentage was 83 and 100 percent respectively. These results are consistent and generally in agreement with the expectation that the percentage removal of a pollutant by ozonation may be increased either by increasing the influent gaseous ozone concentration, or by lowering the liquid throughput through the column. Results show similar trend during experiments with copper-complexed cyanide as compared to experiments with free cyanide. However, cyanide removal percentage was lower, and stoichiometric ozone requirement for cyanide degradation higher in case of experiments with copper-cyanide, compared to all corresponding experiments with free cyanide. As per results shown in this dissertation, the by-products of cyanide decomposition include cyanate (CNO^-), ammonia (NH_3) and nitrate (NO_3^-). It is further postulated that cyanide (CN^-) is degraded to cyanate (CNO^-) through interactions with [•OH] radicals by a relatively rapid reaction ($K_{CN^-,\bullet OH} = 8 \times 10^9$ L-mol^{-1}s^{-1}). The cyanate (CNO^-) thus formed again interacts with [•OH] radical through a slower reaction ($K_{CNO^-,\bullet OH} = 4.8 \times 10^7$ L-mol^{-1} s^{-1}) and is ultimately converted to ammonia (NH_3). The slowness of this reaction would explain the accumulation of cyanate (CNO^-) as a by-product of cyanide ozonation. Ammonia (NH_3) formed due to cyanate (CNO^-) degradation is thought to react with hydroxyl [•OH] radicals by a relatively slow reaction ($K_{NH_3,\bullet OH} = 9.7 \times 10^7$ L-mol^{-1} s^{-1}), and is ultimately converted to nitrate (NO_3^-).

CHAPTER I

INTRODUCTION

Ozone is a colorless, pungent smelling gas with high oxidative power, which has been used for over a hundred years in water and wastewater treatment for various purposes. These include, disinfection, oxidizing iron and manganese, bleaching of color, destruction of taste and odor compounds, enhancement nitrification, control of trihalomethane formation, destruction of hazardous organic and inorganic chemicals, and for enhancing biodegradation.

Due to its inherent instability, ozone, during application in water or wastewater treatment, must be generated onsite from air or pure oxygen, by using an ozone generator. After generation, gaseous ozone is transferred to the water or wastewater. This transfer process occurs in the 'ozone contactor'. Counter-current continuous flow bubble type ozone contactors are the most common devices used for application of ozone to water. However, comprehensive mathematical modeling of such systems is required for design of efficient contactors that can deliver ozone to the aqueous phase at the desired rate. Ozone transfer efficiency from gas to liquid phase is mainly controlled by physical parameters such as temperature, gas flow rate, ozone partial pressure, and reactor geometry. Chemical parameters such as pH, ionic strength and composition of aqueous solution also affect ozone transfer.

Mass transfer and absorption of ozone into water using bubble contactors have been studied and modeled, with varying degree of success, by several researchers. However, it must be emphasized that these modeling efforts are in the formative stages, and currently no mechanistic model is available to accurately describe the ozone transfer to, and reactions in aqueous phases that occur when gaseous ozone is contacted with water in a continuous counter-current bubble contactors. Under the circumstances, this area remains a popular area for ongoing research, and will be explored further in this dissertation.

Ozone is applied to water for various purposes, as mentioned earlier. One such application, i.e., for destruction of free and copper-complexed cyanide, will be also explored in this dissertation. Cyanide removal from wastewater by ozonation is currently an well-accepted process. References of this process may be found in literature dating back fifty years. However, the initial investigations in this area were exploratory in nature, with little useful information regarding ozone doses required and the consequent rate and extent of cyanide destruction and by-product formation. Later investigations, however, made some useful attempts at generating fundamental kinetic and mechanistic data for the reactions of ozone with free and complexed cyanide. However, such work was also hampered by the incomplete knowledge of aquatic ozone chemistry, especially regarding the importance of the hydroxyl [•OH] radicals produced during ozonation in interactions with cyanide.

The ozone contactor modeling described in this dissertation is distinguished by the comprehensive incorporation aqueous ozone decomposition chemistry concepts in the modeling studies described herein. Additionally, simulation results obtained though mathematical modeling have been experimentally verified. The results of cyanide destruction experiments reported in this dissertation, wherever possible, have been explained in terms of the current understanding of aqueous ozone chemistry and interactions of aqueous radical species formed on ozonation with cyanide and other solutes present in water.

CHAPTER II

BACKGROUND

2.1 Ozonation in Water and Wastewater Treatment

Ozone is a colorless, pungent smelling gas. Its oxidation potential is 2.07 volts, which is the highest among all the common oxidants used in water/wastewater treatment. Ozone has been used for over a hundred years in water and wastewater treatment for various purposes. These include, disinfection (Katzenelson and Shuval 1974, Rice et al., 1981), oxidizing iron and manganese, bleaching of color (Rice et al., 1981, O'Donovan 1965, Edwards and Amirtarajah 1985), etc. In addition, ozone has been used for reducing taste and odor compounds (Sontheimer 1985, Rice et al., 1981), to enhance nitrification (Sontheimer et al., 1978), to control trihalomethane formation (Trussel and Umphres, 1978), and for enhancing biodegradation (Benitez et al., 2001).

2.1.1 Ozone generation

Ozone is a meta-stable molecule produced from elemental oxygen. The overall reaction for ozone formation is endothermic (Langlais et al., 1991),

$$3O_2 \rightleftarrows 2O_3 \quad ; \quad \Delta H = +284.5 \text{ kJ/mole} \qquad \text{Equation 2.1}$$

hence production of ozone from oxygen requires input of energy. Due to its inherent instability, ozone, during application in water or wastewater treatment, must be generated onsite from air or pure oxygen using an ozone generator. Theoretically, 2960 J of energy is required to produce 1 gm of ozone (Langlais et al., 1991). However, the actual efficiency of ozone generators, which depend on a variety of factors, is much less than this.

The working principle of an ozone generator is as follows. A silent electrical discharge known as corona discharge is maintained between two electrodes by applying high voltage across the electrodes. A dielectric material made of glass, and an air gap separates these electrodes. Pure oxygen or air is passed through this air gap, where due to the high voltage, oxygen molecules ionize and are partially converted to ozone (Langlais et al., 1991).

The three main criteria that define an ozone generator are, 1). Ozone generation capacity (expressed in units such as Kg O_3 generated per day), 2). Ozone concentration in the product gas (expressed in units such as percent by weight or g O_3 produced per m^3 of product gas at NTP), and 3). Energy requirement (expressed in units such as KW-h/Kg O_3). All the three above values are a function of operating parameters such as the type of feed gas (either air or pure oxygen), gas throughput through the ozonator, and the voltage applied for ozone production. Ozone generation capacity or percent ozone production for a particular ozone generator is often plotted as a function of the operating parameters mentioned above for the preparation of characteristic ozone generation curves for ozone generators. Such curves are essential for choosing appropriate ozonation doses for water and wastewater treatment.

2.1.2 Ozone Application to Water and Wastewater

As described above, for application to water and wastewater treatment, gaseous ozone is generated onsite using ozone generator. After generation, gaseous ozone is transferred to the water or wastewater. This transfer process occurs in the 'ozone contactor'.

2.1.2.1 Types of Ozone Contactors

A number of techniques are currently available, and more are being developed for efficient dissolution of ozone into aqueous solutions to be treated by ozonation. A review of various systems installed commercially indicate that fine bubble diffusion systems with the water and gas flowing in the counter current mode is the most common, especially in the United States and also in Europe. (Langlais et al., 1991)). Turbine contacting systems (both aspirating and submerged) have been used for in some treatment plants for ozone dissolution in water. However, the energy requirement of such systems, at 5 W-h/g ozone is considered to be high (Langlais et al., 1991). Injector or static-mixer type ozonation devices are quite common in Europe and Canada, with the Choisy-le-Roi water treatment plant in Paris being the prime example (Langlais, et al., 1991)). Other ozone contacting devices include packed columns, spray contact chambers and some new and patented devices (Langlais et al., 1991).

2.1.2.2 Modeling Ozone Mass Transfer from Gas to Liquid Phase

As mentioned in the last section, counter-current continuous flow bubble type ozone contactors are the most common devices used for application of ozone to water. However, comprehensive mathematical modeling of such systems is required for design of efficient contactors that can deliver ozone to the aqueous phase at the desired rate. The results of these efforts towards development of mechanistic model for bubble type ozone contactors are discussed below.

Ozone transfer efficiency from gas to liquid phase is mainly controlled by physical parameters such as temperature, gas flow rate, ozone partial pressure, and reactor geometry (Sotelo et al., 1989, Langlais et al., 1991). Chemical parameters such as pH, ionic strength and composition of aqueous solution also affect ozone transfer (Sotelo et al., 1989). The effect of physical parameters can be adequately represented by a partition coefficient, e.g., Henry's coefficient, for describing ozone distribution between solid and liquid phase, and a mass transfer coefficient (Beltran et al., 1997). The effect of chemical parameters can be represented by an adequate description of ozone decomposition in the aqueous phase (Langlais et al., 1991).

Mass transfer and absorption of ozone into water using bubble contactors have been studied and modeled, with varying degree of success, by several researchers (Anselmi et al., 1984; Roustan et al., 1987; Laplanche et al., 1991, Bin, 1995, Zhou and Smith, 2000 and Wu and Masten, 2001). Among them and others, many researchers have developed models for semi-batch reactors (Wu and Masten, 2001), others have neglected ozone decomposition in aqueous phase (Anselmi et al., 1984), and others have neglected ozone decomposition in gas phase (Roustan et al., 1987). It must be emphasized at this point that these modeling efforts are in the formative stages, currently no mechanistic model is available to accurately describe the ozone transfer to, and reactions in aqueous phases that occur when gaseous ozone is contacted with water in a continuous counter-current bubble contactors. Under the circumstances, this area remains a popular area for ongoing research.

2.1.3 Ozone Decomposition in Pure Water

The decomposition of ozone in pure water has been studied extensively (e.g., Roth and Sullivan 1983, Staehelin and Hoigne 1982). This decomposition is initiated by hydroxyl ions (Figure 2.1). The chain of reaction is cyclic with formation of [•OH] as one of the steps. This cyclic ozone decomposition reaction can be slowed or hastened depending on the types of solutes present in water. The hydroxyl radicals react with certain solutes to form $\bullet O_2^- / \bullet HO_2$ radicals (Figure 2.2). These radicals react with ozone at a much faster rate than OH^- ions (1.6×10^9 $M^{-1}s^{-1}$ vs 70 $M^{-1}s^{-1}$, Staehelin and Hoigne 1985). Thus the decomposition of ozone is accelerated. Such solutes are known as promoters. In the process the promoters are oxidized. Other solutes react with hydroxyl radicals to form products that do not ultimately yield $\bullet O_2^- / \bullet HO_2$ and hence terminate the chain reaction of decomposition of ozone. These solutes are termed scavengers (e.g., alkyl groups, bicarbonate and carbonates). A complete description of the ozone decomposition process is given in Figures 2.1 and 2.2. Various elements of the reaction schemes presented in the above figures have been studied in detail by various researchers (Peleg 1976, Hoigne and Bader 1976, Hoigne and Bader 1975, Hoigne and Bader 1983a and 1983b, Hoigne et al., 1985, Hoigne and Bader 1979, Glaze et al., 1987 and Yurteri 1988).

2.1.4 Reactions of Molecular Ozone with Organic Solutes

The reaction of molecular ozone with organic compounds is very selective in spite of its high oxidation potential. The reaction of molecular ozone with organic compounds can take place by 1-3 dipolar cycloaddition, electrophilic attack or nucleophilic attack (Bailey 1972, Dore 1985). Ozone behaves as a dipole, resulting in 1-3 cycloaddition on unsaturated bonds, and thereby forming ozonides. These ozonides subsequently decompose rapidly into aldehydes, ketones, acids and alcohols in accordance with the Criegee ozonolysis mechanism (Bailey 1978). Electrophilic attack by ozone occurs mostly at the high electron density sites of aromatic compounds. This results in the opening of the aromatic ring and leads to the formation of compounds with carboxyl and carbonyl groups. Nucleophilic attack by ozone on the electron deficient sites is not very prevalent and hence not widely reported. As mentioned above, only compounds of

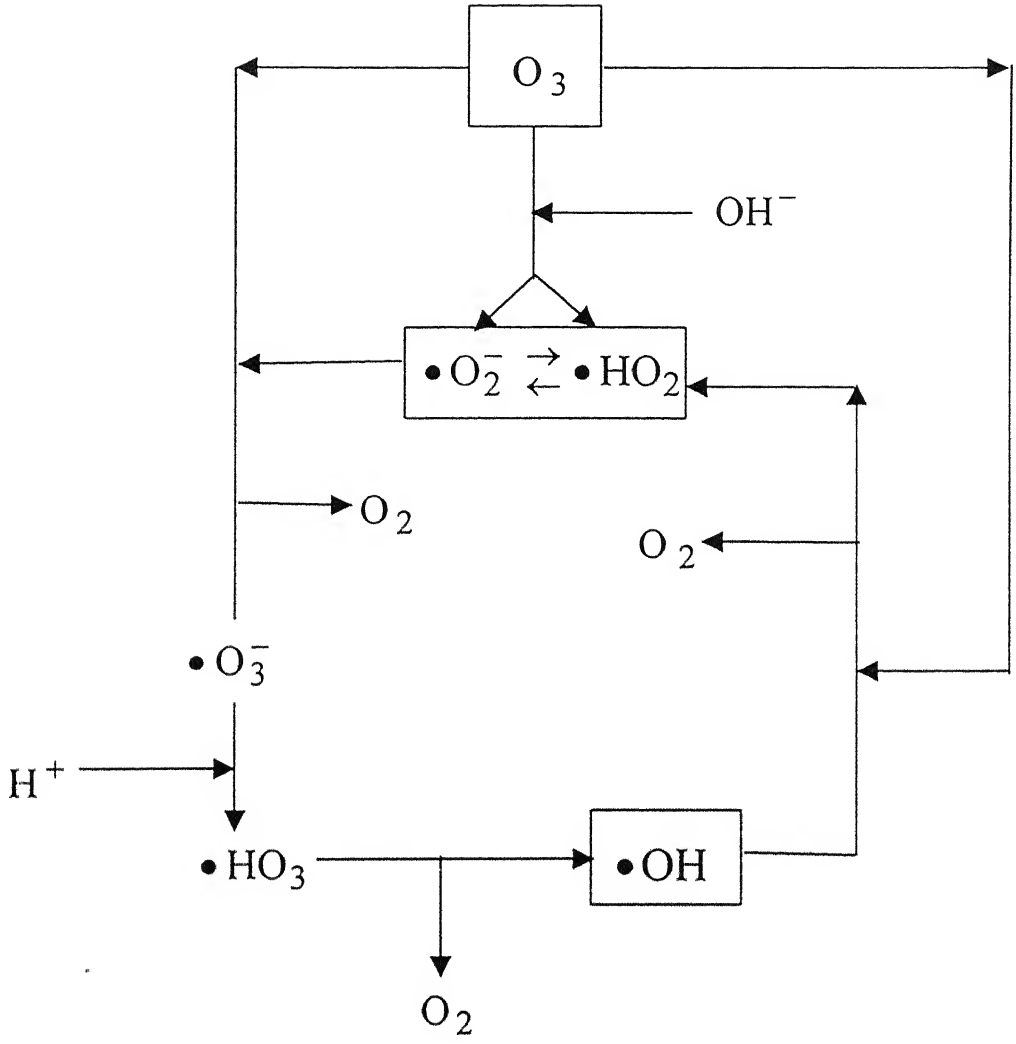

Figure 2.1 Ozone Decomposition Scheme in Pure Water
(As per Staehelin and Hoigne, 1985)

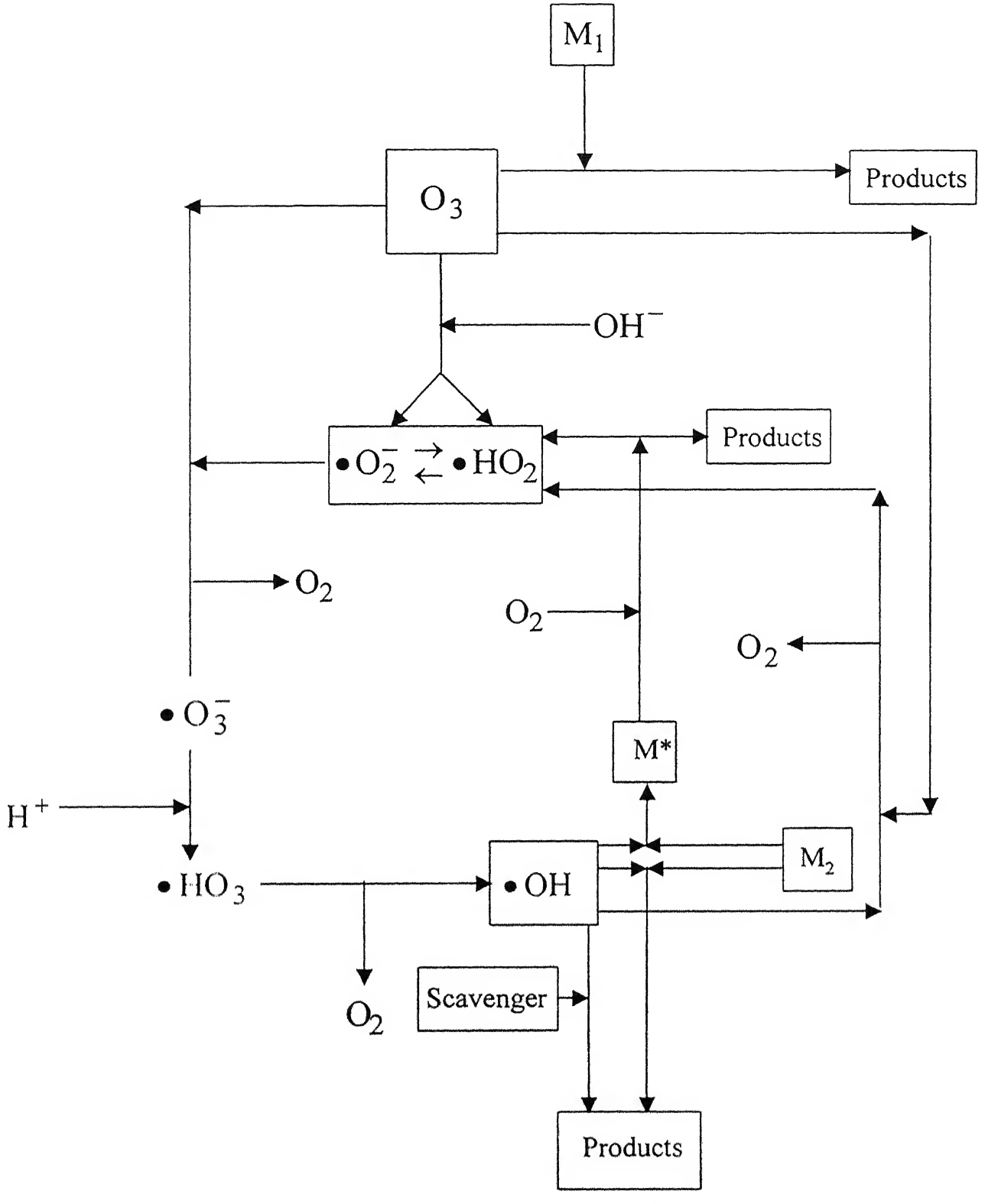

Figure 2.2 Ozone Decomposition Scheme in Water in Presence of Scavenger and Solutes
(As per Staehelin and Hoigne, 1985)

certain types react quickly with molecular ozone. Most of these compounds are nucleophilic, including non-halogen substituted olefins, phenols and phenate ions, polynuclear aromatic hydrocarbons, non protonated amines and thio compounds.

2.1.5 Reaction of Hydroxyl Radicals with Organic and Inorganic Solutes

However, aqueous ozone can be very unstable and under certain conditions it decomposes rapidly in water to produce [•OH] radicals (see section 2.1.3). These [•OH] radicals are more indiscriminate in their reactions with various solutes in water than is molecular ozone. The compounds that would only be attacked by the radical mechanism have fewer reactive functional groups such as, aliphatic hydrocarbons, carboxylic acids, benzene, chlorobenzenes, nitrobenzene and trichloroethylene.

2.2 Cyanide Toxicity and Removal

Various industrial processes such as metal plating and finishing, photographic bleaching, iron and steel manufacturing, etc., produce substantial amounts of wastewater containing high concentration of free and metal complexed cyanide. Both free and complexed cyanide is known to be toxic, both to humans and the flora and fauna in the natural water bodies receiving cyanide-laden wastewater. Consequently destruction of cyanide in wastewater is mandatory before the discharge into natural water bodies.

2.2.1 Cyanide Toxicity

Many forms of cyanide are toxic to humans. Hydrogen cyanide has a time-average exposure limit of 10 ppm for 8 hours (Sax, 1989). Most of the inorganic salts of cyanide have exposure limits of a few parts per million. Only 0.1 to 0.3 grams of free cyanide is sufficient to kill human beings (EPA, 2000). Exposure can occur by absorption through the skin, by inhalation of dusts or gas, or by ingestion. Human exposure toxicity is typically acute rather than chronic. Exceeding exposure levels can result in disorientation, dizziness and nausea. Cyanide poisoning occurs by blocking blood oxygen transfer, which can result in death by asphyxia.

Free cyanide is even more toxic for fish (Benefield et al., 1982). As per Dobson (1947), 0.1 ppm of free cyanide is fatal to some fish. As regards to inhibitory effects on microorganisms, Gurnham et al. (1944) reported that 2mg/L concentration of cyanide in wastewater had an adverse effect on nitrification in trickling filters during wastewater treatment.

Metal-cyanide complexes, while less toxic than free cyanide, are also a cause for concern. Zinc and cadmium complexes of cyanide are unstable and very toxic, while iron and nickel complexes of cyanide are more stable and hence less toxic (Benefield et al. 1982). Pablo et al. (1997) investigated the effect of sodium cyanide and iron cyanide complexes on the unicellular diatom Nitzchia Closterium. The conclusion of this study was that iron cyanide complexes were less toxic than sodium cyanide complexes for these organisms. The effect of a metal plating waste containing chromium, copper, nickel, zinc and cyanide on sewage treatment was studied by Tarvin (1956). Results showed that this mixture had a detrimental effect on the ability of activated sludge to remove BOD from sewage.

2.2.2 Cyanide Removal from Wastewater

Of all the methods for destroying cyanides, the alkaline-chlorination method is most popular (EPA, 2000; Patterson, 1985). Alkaline-chlorination is a two step process, with cyanide (CN^-) being converted to cyanate (CNO^-) in the first step. This process is relatively fast, with complete conversion occurring within 20 minutes. Cyanogen chloride ($CNCl$), which is a very toxic gas, is formed as an intermediate in the above process. However, this gas is very soluble in water, and hence is unlikely to be stripped to air under normal circumstances. Nonetheless, in cases where the reaction is slow due to pH not being sufficiently high, it may persist in solution. Hence alkaline-chlorination process must be carried out in closed reactors with proper venting to the atmosphere. The second step involves the conversion of cyanate (CNO^-) to nitrogen (N_2) gas and carbonate (CO_3^{--}). This process is relatively slow, and a reaction time of 40-60 minutes is not uncommon for complete conversion to occur. Another drawback of this process is

that excess chlorine has to be added to facilitate the destruction of cyanide. Hence the wastewater after cyanide destruction is high in residual chlorine, which must be quenched by addition of suitable quenching agents like sodium sulfite (Na_2SO_3).

Destruction of metal-cyanide complexes by alkaline chlorination (EPA, 2000) is dependent on the strength of the binding between the metal and cyanide (CN^-). Cyanide complexes with cadmium, copper and zinc are destroyed readily by alkaline chlorination. Destruction of cyanide complexes with cobalt, iron, gold, nickel and silver are kinetically limited. Iron complexes of cyanide are not amenable to chlorination. Many researchers have reported studies involving degradation of metal-cyanide complexes. The include Wise (1948), who used chemical precipitation method in a batch system using ferrous sulfate, lime and chlorine to remove chromium and cyanide in wastewater. Balden (1959) has reported a method for treatment of industrial process waste containing chromium and cyanide at Chrysler corporation, where the chromium was allowed to precipitate as chromic hydroxide by the addition of sodium meta-bi-sulfite powder under acidic conditions. The free cyanide bearing wastes were then treated with sodium hypo-chlorite solution in alkaline conditions, and then the mixed effluent was drained to the city sewer. Garrett et al. (1958) at Trans World Airlines (TWA) chemical waste disposal plant suggested a similar method as above for destruction of metal-complexed cyanide waste. Here, ferrous sulfate was used in place of sodium meta-bi-sulphide for chromium precipitation, and chlorine gas and caustic soda in place of sodium hypo-chloride for the oxidation of cyanide.

Other commonly practiced methods for destruction of cyanide recommended by EPA (EPA, 2000) and others include, oxidation by hydrogen peroxide, oxidation by ozone, degradation by UV radiation, destruction by other advanced oxidation processes (AOPs) like UV/O_3, $UV/O_3/H_2O_2$, electrochemical oxidation (Szpyrkowicz, 1998), thermal oxidation, and acidification/acid hydrolysis.

Other less common methods for cyanide destruction in wastewater include precipitation with ferrous salts (Hartinger, 1994); adsorption on catalyzed activated carbon (Patterson,

1985); the 'Kastone' process (Patterson, 1985); destruction with 'Caro's' acid (Eilbeck, 1987, Hartinger, 1994). Other methods described in the literature include destruction with aldehydes (Eilbeck, 1987); destruction with SO_2/air (Inco, 1993); wet air oxidation (Li and Lou, 2000) and destruction with Fention's reagent (Eilbeck, 1987).

2.2.3 Cyanide Removal By Ozonation

Cyanide removal from wastewater by ozonation is currently an well-accepted process. References of this process may be found in literature starting more than fifty years ago (Tyler et al., 1949; Streebin et al., 1981; Walker and Zabban, 1953; Selm, 1959; Khandelwal et al., 1959; Sondak and Dodge, 1961; Matsuda et al. 1975; Zeelvalkink et al. 1979; Rowley and Otto, 1980). However, the initial investigations in this area were exploratory in nature, with little useful information regarding ozone doses required and the consequent rate and extent of cyanide destruction and by-product formation. The main findings from the above research was that ozone could degrade free cyanide and some metal-complexed cyanide quite readily, cyanide degradation was faster at higher pH values, and the main by-product of such ozonation was cyanate (CNO^-), which was in turn degraded relatively slowly by ozonation to ammonia (NH_3) and nitrate (NO_3^-).

Gurol et al. (1985) made a commendable attempt in generating fundamental kinetic and mechanistic data for the reactions of ozone with free and complexed cyanide, by distinguishing between the mass transfer of ozone and oxidation and decomposition reactions of ozone. However, this work was hampered by the incomplete knowledge of aquatic ozone chemistry prevalent at the time, especially regarding the importance of the hydroxyl [•OH] radicals produced during ozonation in interactions with cyanide.

CHAPTER III
SCOPE AND OBJECTIVES

Application of ozone for achieving various objectives in water and wastewater treatment has become quite common in recent years in many countries. Consequently the scope of the commercial application of the technology and associated research opportunities in the field of application of ozonation for water and wastewater treatment is also very vast. The research described in this dissertation however focuses on two very specific problems in this field. Specifically, the objectives of the research described in this dissertation are,

- Mechanistic modeling of continuous flow counter current ozone contactor incorporating concepts describing rate and extent of ozone mass transfer from gaseous to aqueous phases, and comprehensive consideration of ozone decomposition reactions in the aqueous phase.

- Experimental verification of model simulation results by performing well-controlled experiments using a continuous flow counter current ozone contactor, for obtaining the necessary data under varying physical and chemical conditions.

- Conducting experimental studies under various physical and chemical conditions for the determination of the rate and extent of degradation of free and copper-complexed cyanide by ozonation and monitoring the consequent evolution of ozonation by-using the same ozone contactor as described above.

- Explanation of the cyanide degradation and by-product formation results in terms of the current understanding of aqueous ozone chemistry and interactions of aqueous radical species formed on ozonation with cyanide and other solutes present in water.

CHAPTER IV

SIMULATION OF OZONE MASS TRANSFER AND REACTION IN A COUNTER-CURRENT CONTINUOUS FLOW BUBBLE CONTACTOR CONTAINING PURE WATER

4.1 Introduction

The rate of mass transfer of ozone from gas to the liquid phase is dependent on various physical parameters such as temperature, liquid and gas flow rates, ozone partial pressure, type of diffusers, and reactor geometry, and chemical parameters such as pH, ionic strength and composition of the aqueous solution. Characterization of ozone mass transfer is further complicated by the fact that aqueous ozone is very reactive and under certain conditions, likely to be consumed quickly even in pure water. Ozone mass transfer, as applicable for water and wastewater treatment operations, is effected in 'ozone contactors'. Among the ozone contactors currently in use commercially, the continuous-flow counter-current bubble contactor is among the most common. As described in section 2.1.2.2, comprehensive mathematical modeling of such systems is required for design of efficient contactors that can deliver ozone to the aqueous phase at the desired rate, and hence this is an area for ongoing research.

An attempt has been made in this chapter to mathematically simulate ozone mass transfer and absorption to pure water contained in a continuous-flow counter-current bubble contactor. For the purpose of this simulation, both the rate and extent of ozone mass transfer from the gas to the liquid phase and degradation of ozone in the liquid phase have been taken into consideration. Ozone mass transfer has been described using Henry's law and the Lewis-Whitman two-film theory for mass transfer. Ozone reactions in aqueous phase have been described in terms of appropriate rate expressions that describe the formation of radical species due to interactions of ozone in water.

4.2 Reactor Configuration

A schematic of the reactor to be simulated is shown in Figure 4.1. Water is introduced into the reactor from the top and withdrawn at the same rate from the bottom. Oxygen gas, containing 1-2 percent ozone is introduced into the reactor from the bottom through a porous ceramic plate such that the small bubbles are released into the water column to facilitate mass transfer.

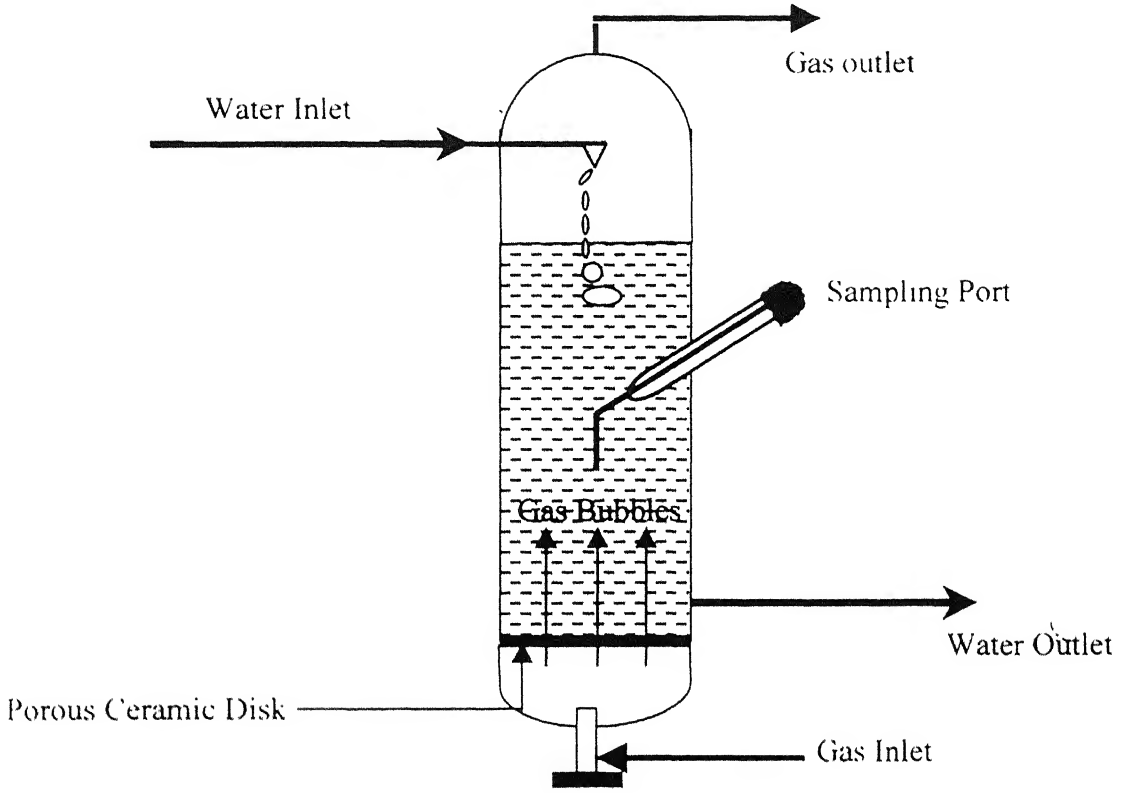

Figure 4.1 Schematic of the Reactor

The vital reactor characteristics are presented in Table 4.1. It is assumed that due to the agitation caused by gas bubbles and due to low length: diameter ratio, the aqueous contents of the reactor are well mixed. Tracer studies conducted to verify this assumption, and presented in chapter VI show this to be essentially true. Similar assumption is made about the gaseous contents of the reactor, though the validity of this assumption is not experimentally verified. However, errors introduced in this regard are considered to be small considering the relatively low length: diameter ratio of the reactor.

Table 4.1 Reactor Characteristics

Reactor Shape	Cylindrical
Height, H_0, cm	39
Diameter, D, cm	6.4
Cross-Sectional Area, A, m^2	3.22×10^{-3}
Depth of Liquid, H, cm	31
Average size of gas bubble, d, mm	1
Length: Diameter Ratio	4.84

4.3 Partitioning of Ozone Between Gas and Liquid Phase

Henry's Law describes partitioning of ozone between gas and liquid phases. Accordingly,

$$P_{[O_3]} = H_{[O_3]}.X_{[O_3]} \qquad \text{Equation 4.1}$$

Where, $P_{[O_3]}$ is the partial pressure of ozone in the gaseous phase, expressed in atmospheres, $X_{[O_3]}$ is the saturation mole fraction of ozone in the aqueous phase, and $H_{[O_3]}$ is the Henry's constant for ozone, expressed in atmospheres.

4.3.1 Dependence of Henry's Constant on Temperature

As per Henry's Law expression above, the solubility of ozone in aqueous phase is proportional to the partial pressure of ozone in the gaseous phase, with the Henry's constant ($H_{[O_3]}$) being the constant of proportionality. The value of Henry's constant is a function of temperature as shown in Table 4.2.

Table 4.2 Variation of Henry's Law Constant for Ozone with Temperature (Adapted from Langlais, et al. 1991)

Temperature, °C	0	5	10	15	20	25	30	35
Henry's Constant, $H_{[O_3]}$, atm.	1945	2490	3190	4200	5190	6555	8302	10375

As per values given in this table, at low temperatures, the value of $H_{[O_3]}$ is lower than at higher temperatures. This would suggest that for a particular $P_{[O_3]}$, ozone solubility would be higher at lower temperatures than at higher temperatures.

4.3.2 Calculation of Solubility Ratio (S) and its Dependence on Temperature

Henry's law can also be written in terms of solubility ratio (S), which is the ratio of saturation ozone concentration in aqueous phase to the gaseous ozone concentration, when both concentrations are expressed in mg/L (or moles/L). In mathematical terms,

$$S = \frac{[O_3]_l^s \text{ in mg/L (or moles/L)}}{[O_3]_g \text{ in mg/L (or moles/L)}} \qquad \text{Equation 4.2}$$

Solubility ratio for the reactor under question was calculated at various temperatures for an influent gaseous ozone concentration of 30 mg/L and an inlet air pressure of 1.1 atmospheres. These calculations are shown in Table 4.3.

Table 4.3 Calculation of Solubility Ratio (S)

Parameter		Value			
Inlet Pressure, atm.		1.10			
Volume of 1 mole of air, L	Temp. = 30°C	22.58727			
	Temp. = 25°C	22.21455			
	Temp. = 20°C	21.84182			
	Temp. = 15°C	21.46909			
Moles of air in 1 L, moles	Temp. = 30°C	4.83E-02			
	Temp. = 25°C	4.91E-02			
	Temp. = 20°C	4.99E-02			
	Temp. = 15°C	5.08E-02			
Gas Phase Ozone Concentration, $[O_3]_g$		mg/L	moles/L	Mole Fraction, $Y_{[O_3]}$	Partial Pressure, $P_{[O_3]}$, atm
	Temp. = 30°C	30	6.25E-04	1.29E-02	1.42E-02
	Temp. = 25°C	30	6.25E-04	1.27E-02	1.40E-02
	Temp. = 20°C	30	6.25E-04	1.25E-02	1.38E-02
	Temp. = 15°C	30	6.25E-04	1.23E-02	1.35E-02
Henry's Constant, $H_{[O_3]}$, atm	Temp. = 30°C	8302			
	Temp. = 25°C	6555			
	Temp. = 20°C	5190			
	Temp. = 15°C	4200			
Saturation Liquid Phase Ozone Concentration, $[O_3]_l^s$		mg/L	moles/L	Mole Fraction, $X_{[O_3]}$	
	Temp. = 30°C	4.57	9.52E-05	1.71E-06	
	Temp. = 25°C	5.69	1.19E-04	2.14E-06	
	Temp. = 20°C	7.07	1.47E-04	2.65E-06	
	Temp. = 15°C	8.58	1.79E-04	3.22E-06	
Solubility Ratio, S	Temp. = 30°C	0.1523			
	Temp. = 25°C	0.1897			
	Temp. = 20°C	0.2355			
	Temp. = 15°C	0.2861			

As per these calculations, the solubility ratio, and hence the saturation aqueous ozone concentration shows a decrease with increasing temperature for a particular influent gaseous ozone concentration. The solubility ratio, as calculated below plays an important part in the formulation of kinetic expressions for modeling ozone mass transfer and reactions, which are described in later sections of this chapter.

4.4 Rate of Ozone Mass Transfer

Ozone mass transfer from the gaseous to the aqueous phase may be expressed by an equation of the form,

$$[O_3]_g \underset{k_1'}{\overset{k_2'}{\rightleftharpoons}} [O_3]_l \qquad \text{Equation 4.3}$$

where $[O_3]_g$, and $[O_3]_l$ are the ozone concentrations in the gaseous and aqueous phases respectively. Based on the above equation, rate of ozone transfer from the gaseous to the liquid phase may be expressed as,

$$\frac{d[O_3]_l}{dt} = k_1'.[O_3]_g - k_2'[O_3]_l \qquad \text{Equation 4.4}$$

It is also known that, $S.[O_3]_g = [O_3]_l^s$, where, S and $[O_3]_l^s$ are as defined in section 4.3.2. Substituting these values in Equation 4.4b

$$\frac{d[O_3]_l}{dt} = \frac{k_1'}{S}.[O_3]_l^s - k_2'[O_3]_l \qquad \text{Equation 4.5}$$

Again, as per Lewis-Whitman two film theory for describing the same mass transfer of ozone between gas and liquid phases,

$$\frac{d[O_3]_l}{dt} = K_L.a.\left\{[O_3]_l^s - [O_3]_l\right. \qquad \text{Equation 4.6}$$

Hence, comparing equations 4.4c and 4.4d, it can be deduced that the kinetic constants k_1 and k_2 can be expressed in terms of $K_L.a$ as follows,

$$k_1' = S.\,K_L.a \qquad \text{Equation 4.7}$$

$$k_2' = K_L.a \qquad \text{Equation 4.8}$$

4.4.1 Calculation of $K_L.a$

At 20°C the diffusion constant of ozone, $D_{O_3} = 1.74 \times 10^{-9}\ m^2/s$. Further, this value can be corrected for temperature by using the Nernst-Einstein relationship, which states that, $D_{O_3}.\mu/T = constant$. Hence, diffusion constant of ozone at various temperatures was calculated as shown in Table 4.4.

Table 4.4 Variation of Diffusivity Constant of Ozone, D_{O_3}, with Temperature

T, °C	D_{O_3}, m^2/s	μ, $N.s/m^2$	$D_{O_3}.\mu/T = constant$
30	2.26×10^{-9}	7.98×10^{-4}	5.95×10^{-15}
25	1.99×10^{-9}	8.90×10^{-4}	5.95×10^{-15}
20	1.74×10^{-9}	1.00×10^{-3}	5.95×10^{-15}
15	1.50×10^{-9}	1.14×10^{-3}	5.95×10^{-15}

According to Masschelein (1982), in a static water column through which ozonated air is bubbled, the following relationship applies, $K_L = 1.13.\sqrt{D_{O_3}.\frac{U}{d}}$, where U is the superficial gas velocity in m/s and d is the gas bubble diameter. The bubble diameter was assumed to be 1.5 mm for this simulation. Values of K_L at various temperatures calculated using this relationship are given in Table 4.5. Based on the calculated values of K_L and assumed value of bubble diameter, values of $K_L.a$ for various temperatures were calculated as shown in Table 4.5. These $K_L.a$ values were used for subsequent simulation studies. $K_L.a$ values calculated for the ozone mass transfer in the bubble contactor under consideration and presented in Table 4.5 range from $0.399 s^{-1}$ at 30°C to $0.326 s^{-1}$ at 15°C. For comparison, $K_L.a$ for the same reactor was determined experimentally. This was done by assuming that at high pH, the aqueous ozone concentration in the reactor will be zero. Hence, $K_L.a$ can be determined based on experimental determination of influent and effluent gaseous ozone concentration from the reactor. A detailed exposition of this determination is presented in Chapter VI. Comparison of results indicates that the experimental and theoretically determined values are quite close.

Table 4.5 Calculation of $K_L.a$

Parameter		Value
Column Diameter, D, cm		6.4
Column Cross-Sectional Area, A, m^2		3.22×10^{-3}
Gas Flow Rate, Q_g, m^3/s		1.67×10^{-5}
Superficial Velocity, U, m/s		5.18×10^{-3}
Bubble Diameter, d, mm		1.5
K_L, m/s	Temp. 30°C	1.22×10^{-4}
	Temp. = 25°C	1.15×10^{-4}
	Temp. = 20°C	1.07×10^{-4}
	Temp. = 15°C	9.96×10^{-5}
Individual Bubble Volume, v, m^3		1.77×10^{-9}
Bubble Number/m^3 of Gas, N		5.66×10^{8}
Individual Bubble Surface Area, s, m^2		7.07×10^{-6}
Specific Bubble Surface Area, a = (s/v), m^2/m^3		4000
Calculated $K_L.a$ (s^{-1})	Temp. = 30°C	0.399
	Temp. 25°C	0.375
	Temp. = 20°C	0.350
	Temp. 15°C	0.326

4.5 Ozone Reactions in Aqueous Phase

Gaseous ozone applied to the bubble contactor is transferred to the aquatic phase through the mass transfer processes described in the previous sections. However ozone transferred to aqueous phase is not stable and is liable to undergo decomposition. The rate and extent of this decomposition is however dependent on prevalent chemical conditions, i.e., pH, bicarbonate/carbonate alkalinity and the presence of other ozone-consuming species in the aqueous phase. Even when considering a relatively pure aqueous phase, i.e., in the absence of ozone-demanding substances, the rate of ozone decomposition depends on a complex series of reactions involving radical species, as shown in Table 4.6. In such a case the pH and bicarbonate/carbonate alkalinity of the water are the only two variables that control ozone

decomposition. Ozone decomposition reactions may be categorized into various types, i.e., initiation, propagation, scavenging and promotion reactions. These categories will be discussed individually in the sections that follow.

Table 4.6 Ozone Reactions in Pure Water Containing Bicarbonate/Carbonate Alkalinity (NDRL, 2002)

	Reaction	Rate Constant
1.	$O_3 + OH \xrightarrow{k_1} \bullet O_2^- + \bullet HO_2$	$k_1 = 70\ M^{-1}s^{-1}$
2.	$O_3 + HO_2 \xrightarrow{k_2} \bullet O_3^- + \bullet HO_2$	$k_2 = 5.5 \times 10^6\ M^{-1}s^{-1}$
3.	$O_3 + \bullet O_2 \xrightarrow{k_3} \bullet O_3^- + O_2$	$k_3 = 1.6 \times 10^9\ M^{-1}s^{-1}$
4.	$H^+ + \bullet O_3 \xrightarrow{k_4} \bullet HO_3$	$k_4 = 5.2 \times 10^{10}\ M^{-1}s^{-1}$
5.	$\bullet HO_3 \xrightarrow{k_5} \bullet OH + O_2$	$k_5 = 1.1 \times 10^5\ s^{-1}$
6.	$O_3 + \bullet OH \xrightarrow{k_6} \bullet HO_2 + O_2$	$k_6 = 1.1 \times 10^8\ M^{-1}s^{-1}$
7.	$H_2O_2 + \bullet OH \xrightarrow{k_7} \bullet HO_2 + H_2O$	$k_7 = 2.7 \times 10^7\ M^{-1}s^{-1}$
8.	$HO_2 + \bullet OH \xrightarrow{k_8} \bullet O_2^- + H_2O$	$k_8 = 7.5 \times 10^9\ M^{-1}s^{-1}$
9.	$\bullet HO_2 + \bullet OH \xrightarrow{k_9} H_2O + O_2$	$k_9 = 1.0 \times 10^{10}\ M^{-1}s^{-1}$
10.	$\bullet HO_2 + \bullet HO_2 \xrightarrow{k_{10}} H_2O_2 + O_2$	$k_{10} = 8.3 \times 10^5\ M^{-1}s^{-1}$
11.	$H_2O + \bullet HO_2 + \bullet O_2 \xrightarrow{k_{11}} H_2O_2 + O_2 + OH^-$	$k_{11} = 9.7 \times 10^7\ M^{-1}s^{-1}$
12.	$\bullet HO_2 \underset{k_{12}^b}{\overset{k_{12}^f}{\rightleftharpoons}} H^+ + \bullet O_2^-$	$K_{12} = \frac{k_{12}^f}{k_{12}^b} = 10^{-4.8}\ M$
13.	$H_2O_2 \underset{k_{13}^b}{\overset{k_{13}^f}{\rightleftharpoons}} HO_2^- + H^+$	$K_{13} = \frac{k_{13}^f}{k_{13}^b} = 10^{-11.8}\ M$
14.	$H_2O \underset{k_{14}^b}{\overset{k_{14}^f}{\rightleftharpoons}} OH^- + H^+$	$K_{14} = \frac{k_{14}^f}{k_{14}^b} = 10^{-14}\ M^2$
15.	$H_2CO_3^* \underset{k_{15}^b}{\overset{k_{15}^f}{\rightleftharpoons}} HCO_3^- + H^+$	$K_{15} = \frac{k_{15}^f}{k_{15}^b} = 10^{-6.3}\ M$
16.	$HCO_3^- \underset{k_{16}^b}{\overset{k_{16}^f}{\rightleftharpoons}} CO_3^{--} + H^+$	$K_{16} = \frac{k_{16}^f}{k_{16}^b} = 10^{-10.3}\ M$
17.	$HCO_3^- + \bullet OH \xrightarrow{k_{17}} \bullet CO_3^- + H_2O$	$k_{17} = 1.0 \times 10^7\ M^{-1}s^{-1}$
18.	$CO_3^{--} + \bullet OH \xrightarrow{k_{18}} \bullet CO_3^- + OH^-$	$k_{18} = 4.0 \times 10^8\ M^{-1}s^{-1}$
19.	$\bullet CO_3^- + \bullet OH \xrightarrow{k_{19}} HCO_3^- + H_2O_2$	$k_{19} = 3.0 \times 10^8\ M^{-1}s^{-1}$

4.5.1 Initiation Reaction

Reactions involving ozone and other inorganic or organic species, i.e., initiators, which lead to the formation of super-oxide species ($\bullet O_2^-/\bullet HO_2$) are known as initiation reactions. These reactions may be looked upon as the starting step of the aqueous ozone decomposition process. Common initiators in pure water include hydroxyl (OH^-) and hydro-peroxyl (HO_2^-) ions. In impure waters, several organic compounds like glyoxylic acid, formic acid and humic substances may also act as initiators. Equation No. 1 and 2 in Table 4.6 are the common initiation reactions in pure waters, with the former reaction being predominant.

4.5.2 Propagation Reaction

Propagation reactions are of two categories. The first category reactions lead to the formation of hydroxyl ($\bullet OH$) radicals, as shown by Equations 3, 4 and 5 in Table 4.6. As discussed in Chapter II, formation of hydroxyl radicals during ozonation process is an important occurrence, since the hydroxyl radical ($\bullet OH$) species are very reactive and are responsible for oxidizing many impurities present in water. The second category of reactions, as described by equations 10 and 11 lead to the formation of hydrogen peroxide (H_2O_2) through the interaction between super-oxide ($\bullet O_2^-/\bullet HO_2$) species. These reactions are relatively unimportant during ozonation of pure water, but gain importance during combined addition of ozone and hydrogen peroxide (O_3/H_2O_2) or the 'peroxone' process, where initiation of ozone decomposition by Equation No. 2 in Table 4.6 gains prominence.

4.5.3 Promotion Reaction

Promotion reactions are those reactions involving hydroxyl ($\bullet OH$) radicals and other inorganic/organic species, i.e., promoters, through which super-oxide ($\bullet O_2^-/\bullet HO_2$) species may be regenerated. These reactions are important because regeneration of super-oxide species in turn accelerate the ozone decomposition process (see Equation No. 3 in Table 4.6). Reactions shown by Equation Nos. 6, 7 and 8 in Table 4.6 are the common promotion reactions that occur on ozonation of pure water.

4.5.4 Scavenging Reaction

Scavenging reactions are those reactions involving hydroxyl ($\bullet OH$) radicals and other inorganic/organic species, i.e., scavengers, which does not lead to regeneration of super-oxide ($\bullet O_2^- / \bullet HO_2$) species. These reactions are important because non-regeneration of super-oxide species in turn decelerate the ozone decomposition process, and help stabilize ozone in aqueous solutions. In pure water, bicarbonate/carbonate (HCO_3^- / CO_3^{--}) ions are the main scavengers present. In impure waters, other inorganic and organic species may also act as scavengers. Reactions shown by Equation Nos. 9, 17, 18 and 19 in Table 4.6 are the common scavenging reactions that occur on ozonation of pure water.

4.5.5 Equilibrium and Charge Relationships and Electron Balance

In addition to the reactions described above, equilibrium relationships described by Equations 12 to 16 in Table 4.6, which describe equilibrium involving super-oxide radicals (Equation 12), hydrogen peroxide (Equation 13), water (Equation 14), and carbonate system (Equations 15 and 16), are maintained during ozone decomposition in the aqueous phase. Furthermore, all equations in Table 4.6 are balanced in terms of mass, charge and electron. Hence in a system defined by these equations, the above parameters are conserved.

4.5.6 Discussion on Overall Ozone Decomposition

As mentioned earlier, the rate and extent of the pH and the bicarbonate/carbonate alkalinity of the system control ozone decomposition in pure water. Effect of pH on ozone decomposition can be described as follows. At low pH, and hence low [OH^-] concentration, the initiation reaction (Equation 1 in Table 4.6) is hindered due to the low [OH^-] concentration, as compared to systems with high pH. Hence ozone is expected to be more stable in pure water systems at low pH. Effect of bicarbonate/carbonate concentration, i.e., scavenger concentration can be explained as follows. In systems with low scavenger concentration, promotion reactions (Equations 6,7, and 8 in Table 4.6) will predominate, and hence ozone decomposition will be rapid as compared to systems with high scavenger concentrations. In summary, systems at low pH and with high scavenger concentration will afford more stability to aqueous ozone, as compared to systems at high pH and low scavenger concentration.

4.6 Equations Describing Ozone Mass Transfer and Reactions

As per mass transfer relationships presented in section 4.4 and equations describing ozone decomposition presented in Table 4.6, total number of species to be considered for modeling purposes is 15, i.e., $[O_3]_g$, $[O_3]_l$, $[OH^-]$, $[\bullet O_2^-]$, $[\bullet HO_2]$, $[HO_2^-]$, $[\bullet O_3^-]$, $[\bullet HO_3]$, $[\bullet OH]$, $[H_2O_2]$, $[H^+]$, $[H_2CO_3^*]$, $[HCO_3^-]$, $[CO_3^{--}]$, and $[\bullet CO_3^-]$. As stated in section 4.2, it is also assumed that the bubble contactor under consideration is completely mixed both in the aqueous and gaseous phases.

Under the circumstances, for each species to be modeled, a mass balance equation of the type shown below can be written.

$$\begin{Bmatrix}\text{Rate of Species}\\ \text{Accumulation}\end{Bmatrix} = \begin{Bmatrix}\text{Rate of}\\ \text{Species}\\ \text{Input}\end{Bmatrix} + \begin{Bmatrix}\text{Rate of}\\ \text{Species}\\ \text{Formation}\end{Bmatrix} - \begin{Bmatrix}\text{Rate of}\\ \text{Species}\\ \text{Output}\end{Bmatrix} - \begin{Bmatrix}\text{Rate of}\\ \text{Species}\\ \text{Destruction}\end{Bmatrix} + \begin{Bmatrix}\text{Rate of}\\ \text{Mass}\\ \text{Transfer}\end{Bmatrix}$$

Equation 4.9

Such equations for all 15 species mentioned above have been written and are presented in Table 4.7.

4.6.1 Incorporation of Equilibrium Relationships

Unlike the case of irreversible reactions, where only one kinetic rate constant is required to describe the equation, in case of reversible reactions, rates for both the forward and backward reactions are required. However, for reversible reactions, the forward and backward reaction rates may not be available, since such reactions are generally described by an equilibrium constant, which is the ratio of the forward to the backward reaction rate. The procedure adopted for incorporating an equilibrium relationship in mass balance equations was to assign arbitrarily high forward and backward reaction rates, with the constraint that the ratio of the two rates be equal to the corresponding equilibrium constant. Under the circumstances, care must be taken to ensure that the arbitrary values chosen as above are at least an order of magnitude higher than the largest irreversible reaction rates that are encountered. This will ensure that concerned species related through equilibrium relationships remain in equilibrium even while participating in other irreversible reaction.

Table 4.7 Mass Balance Equations for Various Species formed on Ozonation of Pure Water

No.	Species	Rate Input to the Reactor	Rate Produced Inside Reactor	Rate Consumed Inside Reactor	Rate Output From the Reactor	Rate of Mass Transfer
1.	$[O_3]_g$	$Q_g.[O_3]_g^i$	0	0	$Q_g.[O_3]_g$	$-\{k_1'[O_3]_g - k_2'[O_3]_l\}.V$
2.	$[O_3]_l$	0	0	$\{k_1.[O_3].[OH^-] + k_2.[O_3].[HO_2^-] + k_3.[O_3].[\bullet O_2^-] + k_6[O_3].[\bullet OH]\}.V$	$Q_l.[O_3]$	$\{k_1'[O_3]_g - k_2'[O_3]_l\}.V$
3.	$[OH^-]$	$Q_l.[OH^-]_i$	$\{k_{14}^f + k_{18}.[CO_3^{--}].[\bullet OH]\}.V$	$\{k_1.[O_3].[OH^-] + k_{14}^b.[H^+].[OH^-] + k_1.[O_3].[OH^-]\}.V$	$Q_l.[OH^-]$	0
4.	$[\bullet O_2^-]$	0	$\{k_1.[O_3].[OH^-] + k_8.[HO_2^-].[\bullet OH] + k_{12}^f.[\bullet HO_2]\}.V$	$\{k_3.[O_3].[\bullet O_2^-] + k_{11}.[\bullet HO_2].[\bullet O_2^-] + k_{12}^b.[H^+].[\bullet O_2^-]\}.V$	$Q_l.[\bullet O_2^-]$	0
5.	$[\bullet HO_2]$	0	$\{k_1.[O_3].[OH^-] + k_2.[O_3].[HO_2^-] + k_6.[O_3].[\bullet OH] + k_7.[H_2O_2].[\bullet OH] + k_{12}^b.[H^+].[\bullet O_2^-]\}.V$	$\{k_9.[\bullet HO_2].[\bullet OH] + k_{10}.[\bullet HO_2].[\bullet HO_2] + k_{11}.[\bullet HO_2].[\bullet O_2^-] + k_{12}^f.[\bullet HO_2]\}.V$	$Q_l.[\bullet HO_2]$	0

Table 4.7 (Continued)

No.	Species	Rate Input to the Reactor	Rate Produced Inside Reactor	Rate Consumed Inside Reactor	Rate Output From the Reactor	Rate of Mass Transfer
6.	$[HO_2^-]$	0	$\{k_{13}^f.[H_2O_2]\}$	$\{k_2.[O_3].[HO_2^-]+ k_8.[HO_2^-].[\bullet OH]+ k_{13}^b.[H^-].[HO_2^-]\}.V$	$Q_1.[HO_2^-]$	0
7.	$[\bullet O_3^-]$	0	$\{k_2.[O_3].[HO_2^-]+ k_3.[O_3].[\bullet O_2^-]\}.V$	$\{k_4.[H^+].[\bullet O_3^-]\}.V$	$Q_1.[\bullet O_3^-]$	0
8.	$[\bullet HO_3]$	0	$\{k_4.[H^+].[\bullet O_3^-]\}.V$	$\{k_5.[\bullet HO_3]\}.V$	$Q_1.[\bullet HO_3]$	0
9.	$[\bullet OH]$	0	$\{k_5.[\bullet HO_3]\}.V$	$\{k_6.[O_3].[\bullet OH]+ k_7.[H_2O_2].[\bullet OH]+ k_8.[HO_2^-].[\bullet OH]+ k_9.[\bullet HO_2].[\bullet OH]+ k_{17}.[HCO_3^-].[\bullet OH]+ k_{18}.[CO_3^{--}].[\bullet OH]+ k_{19}.[\bullet CO_3^-].[\bullet OH]\}.V$	$Q_1.[\bullet OH]$	0
10.	$[H_2O_2]$	0	$\{k_{10}.[\bullet HO_2].[\bullet HO_2]+ k_{11}.[\bullet HO_2].[\bullet O_2^-]+ k_{13}^b.[H^+].[HO_2^-]+ k_{19}.[\bullet OH].[\bullet CO_3^-]\}.V$	$\{k_7.[H_2O_2].[\bullet OH]+ k_{13}^f.[H_2O_2]\}.V$	$Q_1.[H_2O_2]$	0

Table 4.7 (Continued)

No.	Species	Rate Input to the Reactor	Rate Produced Inside Reactor	Rate Consumed Inside Reactor	Rate Output From the Reactor	Rate of Mass Transfer
11.	$[H^+]$	$Q_1.[H^+]_i$	$\{k^f_{12}.[\bullet HO_2]+ k^f_{13}.[H_2O_2]+ k^f_{14}+ k^f_{15}.[H_2CO^*_3]+ k^f_{16}.[HCO^-_3]\}.V$	$\{k_4.[H^+].[\bullet O^-_3]+ k^b_{12}.[H^+].[\bullet O^-_2]+ k^b_{13}.[H^+].[HO^-_2]+ k^b_{14}.[H^+].[OH^-]+ k^b_{15}.[H^+].[HCO^-_3]+ k^b_{16}.[H^+].[CO^{--}_3]\}.V$	$Q_1.[H^+]$	0
12.	$[H_2CO^*_3]$	$Q_1.[H_2CO^*_3]$	$\{k^b_{15}.[H^+].[HCO^-_3]\}.V$	$\{k^f_{15}.[H_2CO^*_3]\}.V$	$Q_1.[H_2CO^*_3]$	0
13.	$[HCO^-_3]$	$Q_1.[HCO^-_3]$	$\{k^f_{15}.[H_2CO^*_3]+ k^b_{16}.[H^+].[CO^{--}_3]+ k_{19}.[\bullet OH].[\bullet CO^-_3]\}.V$	$\{k^b_{15}.[H^+].[HCO^-_3]+ k^f_{16}.[HCO^-_3]+ k_{17}.[HCO^-_3].[\bullet OH]\}.V$	$Q_1.[HCO^-_3]$	0
14.	$[CO^{--}_3]$	$Q_1.[CO^{--}_3]_i$	$\{k^f_{16}.[HCO^-_3]\}.V$	$\{k^b_{16}.[H^+].[CO^{--}_3]+ k_{18}.[CO^{--}_3].[\bullet OH]\}.V$	$Q_1.[CO^{--}_3]$	0
15.	$[\bullet CO^-_3]$	0	$\{k_{17}.[\bullet OH].[HCO^-_3]+ k_{18}.[\bullet OH].[CO^{--}_3]\}.V$	$\{k_{19}[\bullet OH].[\bullet CO^-_3]\}.V$	$Q_1.[\bullet CO^-_3]$	0

4.6.2 Mass, Charge and Electron Balance

All equations presented in Table 4.6, and used for the subsequent development of mass balance equations presented in Table 4.7 are consistent in terms of mass, charge and electron balance. Hence no separate equations specifying such balances are required for obtaining consistent solution of these equations. Simulation results presented in later sections of this chapter indicate that such solutions are adequate in these respects.

4.6.3 Unsteady and Steady State Solutions

In case of unsteady state solution of the mass balance equations presented in Table 4.7 is desired, the left side of each mass balance equation will be of the form, $V.\frac{d[M]}{dt}$, where V is the reactor volume, and [M] is the species concentration. This will result in 15 coupled differential equations, with 15 unknowns, which may be solved by numerical techniques like the fourth order Runge-Kutta method. In case of steady-state solutions of the mass balance equations, the left side of each equation presented in Table 4.7 will reduce to zero. This will result in 15 non-linear coupled simultaneous equations that may be solved by appropriate numerical techniques. In most cases, obtaining solution of the unsteady state problem for a sufficiently long time period starting from zero time will result in species concentrations, which are virtually invariant with time. Species concentration values corresponding to such conditions may be taken as the 'steady-state' values. Under such circumstances, separate solution of the 'steady-state' problem may not be necessary.

4.6.4 Initial Conditions

Initial conditions need to be specified only for solving the unsteady state problem. Since the problem consists of solving fifteen first order ordinary differential equations (ODEs), fifteen initial conditions are required. These initial conditions are generally in the form of species concentration of all 15 species being specified at the beginning of the simulation. However, since only steady-state simulations will be emphasized in this dissertation, more detailed discussion about this topic is not warranted.

4.7 Solution Procedure

Both the unsteady and steady-state problem described above were solved using a freely available (Bio) chemical Kinetics Simulation Software called GEPASI 3 (Mendes, 1993). Results obtained from the steady-state simulations using this software will be discussed in the next section.

4.8 Simulation Results

As mentioned earlier, the rate of aqueous ozone decomposition depends on solution pH and scavenger concentration. The effects of changes in these two parameters on ozone decomposition were simulated, and the salient features of these simulations are presented in the sections that follow.

4.8.1 Effect of pH

For the purpose of determining the effect of pH on ozone decomposition, simulations were conducted at three pH values, i.e., 7, 8, and 8.8. The scavenger concentration, i.e., C_T for all three cases was maintained at 1 mM. Salient characteristics of these simulations are presented in Table 4.8. As per these results, at pH 7, the steady-state aqueous ozone concentration was found to be higher than at pH 8 and 8.8. Moreover, comparison with calculated saturation ozone concentration at pH 7 indicated that water was almost saturated with ozone, resulting in a precipitous decline in the rate of mass transfer (see Table 4.8). Consequently, under these conditions, the gaseous ozone concentration effluent from the reactor was almost equal to the influent ozone concentration.

Table 4.8 Simulation of the Dependence of Rate of Ozone Mass Transfer on pH ($Q_l = 25$ mL-min^{-1}; $Q_g = 1$ L-min^{-1}, $K_L.a = 0.4$ s^{-1}, $S = 0.225$, $[O_3]_g^i = 30$ mg/L, $C_T = 1$ mM)

pH	7.0	8.0	8.8
Rate of Ozone Mass Transfer, mg/min	0.12	2.45	13.81
Aqueous Ozone Concentration, mg/L	6.74	6.09	3.09
Saturation Aqueous Ozone Conc., mg/L	6.75	6.19	3.67
Effluent Gaseous Ozone Concentration, mg/L	29.97	27.51	16.30

However, at pH 8.8, the steady-state aqueous ozone concentration was lower than at lower pH values, i.e., pH 7 and 8. Additionally, this value was lower than the saturation ozone concentration at pH 8.8, which provided a driving force for continuous ozone mass transfer into the aqueous phase. Consequently, rate of ozone mass transfer is high under these conditions, and the hence gaseous ozone concentration effluent from the reactor was much lower than influent ozone concentration.

4.8.2 Effect of Scavenger Concentration

For the purpose of determining the effect of scavenger concentration on ozone decomposition, simulations were conducted at three C_T values, i.e., 0.01, 0.1, and 1.0 mM. The pH for all three cases was maintained at 8. Salient characteristics of these simulations are presented in Table 4.9. As per these results, at C_T = 1 mM, the steady-state aqueous ozone concentration was found to be higher than at CT values of 0.1 and 0.01 mM. Moreover, comparison with calculated saturation ozone concentration at C_T = 1.0 mM indicated that water was almost saturated with ozone, resulting in a low rate of mass transfer (see Table 4.9). Consequently, under these conditions, the gaseous ozone concentration effluent from the reactor was high and comparable to the influent ozone concentration.

Table 4.9 Simulation of the Dependence of Rate of Ozone Mass Transfer on Scavenger Concentration (C_T) (Q_l = 25 mL-min^{-1}; Q_g = 1 L-min^{-1}, $K_L.a$ = 0.4 s^{-1}, S = 0.225, $[O_3]_g^i$ = 30 mg/L, pH = 8)

C_T, mM	0.01	0.1	1.0
Rate of Ozone Mass Transfer, mg/min	13.19	8.00	2.45
Aqueous Ozone Concentration, mg/L	3.23	4.60	6.09
Saturation Aqueous Ozone Conc., mg/L	3.78	4.93	6.19
Effluent Gaseous Ozone Concentration, mg/L	16.81	21.93	27.51

However, at C_T = 0.01 mM, the steady-state aqueous ozone concentration was lower than at higher C_T values, i.e., 0.1 and 1 mM. Additionally, this value was considerably lower than the saturation ozone concentration at C_T = 0.01 mM, which provided a large driving force for continuous ozone mass transfer into the aqueous phase. Consequently, rate of ozone mass

transfer is high under these conditions, and the hence gaseous ozone concentration effluent from the reactor was much lower than influent ozone concentration.

4.8.3 Discussion on Simulation Results

Detailed presentation of simulation results include specifying the influent and the steady-state concentration of the 15 species under consideration, i.e., $[O_3]_g$, $[O_3]_l$, $[OH^-]$, $[\bullet O_2^-]$, $[\bullet HO_2]$, $[HO_2^-]$, $[\bullet O_3^-]$, $[\bullet HO_3]$, $[\bullet OH]$, $[H_2O_2]$, $[H^+]$, $[H_2CO_3^*]$, $[HCO_3^-]$, $[CO_3^{--}]$, and $[\bullet CO_3^-]$, that are existing/formed due to interactions of aqueous ozone in the reactor. Such specification for a particular scavenger concentration (C_T = 1 mM), as obtained through mathematical simulation, has been presented in Table 4.10 for pH values of 7, 8 and 8.8. Besides the species concentrations, expressions for carbon balance, charge balance and various equilibria have been provided in the same table in order to demonstrate the strict adherence of the simulation results to these constraints, which serve as a check to the correctness of the simulation results. Similar results at a particular pH (pH = 8) has been presented in Table 4.11 for scavenger concentrations of 0.01, 0.1 and 1 mM.

As described in section 4.5.6, at lower pH values, the initiation of ozone decomposition is hindered due to the low [OH^-] concentration, resulting in increased stability of ozone in such systems, as compared to systems with higher pH. Simulation results presented in Table 4.10, wherein aqueous ozone concentration is shown to be 6.74 mg/L at pH 7 as compared to 3.09 mg/L at pH 8.8, support this analysis. A corollary to the above analysis is the expectation that in systems that afford relative stability to aqueous ozone, ozone decomposition products, e.g., [•OH] radicals should be present in lower concentrations than in systems where ozone is relatively unstable. Simulation results presented in Table 4.10 also show this to be true.

Effect of higher scavenger (i.e., C_T in this case) concentration has been described in section 4.5.6 as a hindrance to promotion of ozone decomposition. Hence systems with higher C_T values are expected to show higher aqueous ozone and lower [•OH] radical concentration as compared to systems with lower scavenger concentration. Simulation results presented in Table 4.11 show such analysis to be true.

Table 4.10 Simulation of the Effect of pH on Ozone Decomposition in Continuous Flow Counter-Current Ozone Contactor (Q_l = 25 mL-min^{-1}; Q_g = 1 L-min^{-1}, $K_L.a$ = 0.4 s^{-1}, S = 0.225)

No.	Species	Units	Inorganic Carbon Concentration, C_T = 1 mM					
			pH 7		pH 8		PH 8.8	
			Influent	Reactor	Influent	Reactor	Influent	Reactor
1.	$[O_3]_l$	mg/L	0	6.74	0	6.09	0	3.09
2.	$[OH^-]$	M	1×10^{-7}	9.952×10^{-8}	1×10^{-6}	9.832×10^{-7}	6.310×10^{-06}	6.64×10^{-6}
3.	$[\bullet O_2^-]$	M	0	2.914×10^{-14}	0	2.156×10^{-12}	0	2.331×10^{-11}
4.	$[\bullet HO_2]$	M	0	1.848×10^{-16}	0	1.388×10^{-15}	0	2.239×10^{-15}
5.	$[HO_2^-]$	M	0	4.757×10^{-13}	0	2.559×10^{-10}	0	4.880×10^{-9}
6.	$[\bullet O_3^-]$	M	0	1.323×10^{-12}	0	1.164×10^{-9}	0	5.281×10^{-8}
7.	$[H^+]$	M	1×10^{-7}	1.005×10^{-7}	1×10^{-8}	1.017×10^{-8}	1.585×10^{-09}	1.506×10^{-9}
8.	$[\bullet HO_3]$	M	0	6.286×10^{-14}	0	5.599×10^{-12}	0	3.760×10^{-11}
9.	$[\bullet OH]$	M	0	2.734×10^{-13}	0	1.725×10^{-11}	0	8.472×10^{-11}
10.	$[H_2O_2]$	M	0	3.016×10^{-8}	0	1.642×10^{-6}	0	4.638×10^{-6}
11.	$[H_2CO_3^*]$	M	1.663×10^{-4}	1.662×10^{-4}	1.947×10^{-5}	1.911×10^{-5}	3.056×10^{-6}	2.701×10^{-6}
12.	$[HCO_3^-]$	M	8.333×10^{-4}	8.289×10^{-4}	9.756×10^{-4}	9.415×10^{-4}	9.664×10^{-4}	8.988×10^{-4}
13.	$[CO_3^{=}]$	M	4.176×10^{-7}	4.135×10^{-7}	4.890×10^{-6}	4.639×10^{-6}	3.056×10^{-5}	2.991×10^{-5}
14.	$[\bullet CO_3^-]$	M	0	4.636×10^{-6}	0	3.477×10^{-5}	0	6.871×10^{-5}
15.	$[O_3]_g$	mg/L	30	29.97	30	27.51	30	16.30
$[O_3]_l^S = S.[O_3]_g$		mg/L	6.75		6.19		3.67	
Charge Balance: [2 + 3 + 5 + 6 + 12 + 2(13) + 14 = 7]			-8.341×10^{-4}	-8.343×10^{-4}	-9.864×10^{-4}	-9.866×10^{-4}	-1.034×10^{-3}	-1.034×10^{-3}
Carbon Balance: [11 + 12 + 13 + 14]			10^{-3} M	10^{-3} M	10^{-3} M	10^{-3} M	10^{-3} M	10^{-3} M
H_2O Equilibrium. [2 x 7]			10^{-14}	10^{-14}	10^{-14}	10^{-14}	10^{-14}	10^{-14}
$H_2CO_3^*/HCO_3^-$ Eq.: [12 x 7 / 11]			5.012×10^{-7}	5.012×10^{-7}	5.012×10^{-7}	5.012×10^{-7}	5.012×10^{-7}	5.012×10^{-7}
$HCO_3^-/CO_3^{=}$ Eq.: [13 x 7 / 12]			5.012×10^{-11}	5.012×10^{-11}	5.012×10^{-11}	5.012×10^{-11}	5.012×10^{-11}	5.012×10^{-11}
H_2O_2/HO_2^- Eq.: [5 x 7 / 10]			--	1.585×10^{-12}	--	1.585×10^{-12}	--	1.585×10^{-12}
$\bullet HO_2/\bullet O_2^-$ Eq.: [3 x 7 / 4]			--	1.584×10^{-5}	--	1.580×10^{-5}	--	1.568×10^{-5}

Table 4.11 Simulation of the Effect of Scavenger Concentration (C_T) on Ozone Decompositio in Continuous Flow Counter-Current Ozone Contactor ($Q_l = 25$ mL-min^{-1}; $Q_g = 1$ L-min^{-1}, $K_L.a = 0.4$ s^{-1}, $S = 0.225$)

No.	Species	Units	pH 8					
			$C_T = 0.01$ mM		$C_T = 0.1$ mM		$C_T = 1$ mM	
			Influent	Reactor	Influent	Reactor	Influent	Reactor
1.	$[O_3]_l$	mg/L	0	3.23	0	4.6	0	6.08
2.	$[OH^-]$	M	1×10^{-6}	9.89×10^{-7}	1×10^{-6}	9.9×10^{-7}	1×10^{-6}	9.83×10^{-7}
3.	$[\bullet O_2^-]$	M	0	2.14×10^{-11}	0	9.20×10^{-12}	0	2.16×10^{-12}
4.	$[\bullet HO_2]$	M	0	1.36×10^{-14}	0	5.88×10^{-15}	0	1.39×10^{-15}
5.	$[HO_2^-]$	M	0	7.98×10^{-11}	0	2.42×10^{-10}	0	2.56×10^{-10}
6.	$[\bullet O_3^-]$	M	0	4.43×10^{-9}	0	2.93×10^{-9}	0	1.16×10^{-9}
7.	$[H^+]$	M	1×10^{-8}	1.01×10^{-8}	1×10^{-8}	1.01×10^{-8}	1×10^{-8}	1.02×10^{-8}
8.	$[\bullet HO_3]$	M	0	2.12×10^{-11}	0	1.40×10^{-11}	0	5.60×10^{-13}
9.	$[\bullet OH]$	M	0	3.05×10^{-10}	0	1.20×10^{-10}	0	1.73×10^{-11}
10.	$[H_2O_2]$	M	0	5.09×10^{-7}	0	1.54×10^{-6}	0	1.64×10^{-6}
11.	$[H_2CO_3^*]$	M	1.95×10^{-7}	1.89×10^{-7}	1.95×10^{-6}	1.89×10^{-6}	1.95×10^{-5}	1.91×10^{-5}
12.	$[HCO_3^-]$	M	9.76×10^{-6}	9.39×10^{-6}	9.76×10^{-5}	9.39×10^{-5}	9.76×10^{-4}	9.42×10^{-4}
13.	$[CO_3^{--}]$	M	4.99×10^{-8}	4.66×10^{-8}	4.99×10^{-7}	4.66×10^{-7}	4.997×10^{-6}	4.64×10^{-6}
14.	$[\bullet CO_3^-]$	M	0	3.73×10^{-7}	0	3.71×10^{-6}	0	3.48×10^{-5}
15.	$[O_3]_g$	mg/L	30	16.81	30	21.93	30	27.51
$[O_3]_l^s = S.[O_3]_g$		mg/L	3.78		4.93		6.19	
Charge Balance: [2 + 3 + 5 + 6 + 12 + 2(13) + 14 = 7]			-1.08×10^{-5}	-1.08×10^{-5}	-9.96×10^{-5}	-9.96×10^{-5}	-9.86×10^{-4}	-9.86×10^{-4}
Carbon Balance: [11 + 12 + 13 + 14]			10^{-5} M	10^{-5} M	10^{-4} M	10^{-4} M	10^{-3} M	10^{-3} M
H_2O Equilibrium: [2 x 7]			10^{-14}	10^{-14}	10^{-14}	10^{-14}	10^{-14}	10^{-14}
$H_2CO_3^*/HCO_3^-$ Eq.: [12 x 7 / 11]			5.012×10^{-7}	5.012×10^{-7}	5.012×10^{-7}	5.012×10^{-7}	5.012×10^{-7}	5.012×10^{-7}
HCO_3^-/CO_3^{--} Eq.: [13 x 7 / 12]			5.012×10^{-11}	5.012×10^{-11}	5.012×10^{-11}	5.012×10^{-11}	5.012×10^{-11}	5.012×10^{-11}
H_2O_2/HO_2^- Eq.: [5 x 7 / 10]			--	1.585×10^{-12}	--	1.585×10^{-12}	--	1.585×10^{-12}
$\bullet HO_2/\bullet O_2^-$ Eq.: [3 x 7 / 4]			--	1.582×10^{-5}	--	1.580×10^{-5}	--	1.580×10^{-5}

CHAPTER V

ANALYTICAL METHODS AND EXPERIMENTAL DESIGN

5.1 Introduction

Analytical methods used in this dissertation have been discussed in some detail in this chapter. In addition, information, including make and model number of various instruments used for various analyses have also been mentioned. This is followed by a detailed description of the experimental setup used for conducting the experiments described in this dissertation. Finally, the procedure followed for conducting the various experiment described in this dissertation are presented.

5.2 Analytical Methods

These section gives a description of the chemicals, glassware, chemical stock solutions, instruments and analytical methods used for the experiments described in dissertation. Mostly, proven analytical methods were used for measuring various parameters. Wherever non-standard methods are used, full description of the method is provided.

5.2.1 Chemicals and Glassware

Reagent grade chemicals were used throughout this research. Triple distilled water, further purified by pre-ozonation was used for the experiments described in this research. All stock solutions and standards were made with distilled or triple distilled water. All glassware used in the experiments was thoroughly cleaned to prevent interference and contamination.

5.2.2 Preparation of Stock Solutions

Stock solution of KCN was prepared by dissolving solid KCN in distilled water maintained at high pH for avoiding formation of HCN gas. Stock solution of copper cyanide was prepared by dissolving commercially available CuCN in KCN solution under strong alkaline conditions.

5.2.3 Ozone Measurement

Gaseous ozone was directly measured using an UV absorbance based ozone-monitoring device (ANSEROS, Ozomat GM-6000-OEM, Germany). Aqueous ozone was measured by the Indigo method (4500-O_3-A, APHA et al. 1995), with the final absorbance of Indigo solution being measured spectrophometrically (Spectronic, 20D+, India) using a 4 cm path length cell. In some cases, where interference was not expected, aqueous ozone concentration was directly measured as follows. UV absorbance of the aliquot containing aqueous ozone was determined at 260 nm using a UV spectrophotometer (Cary 50 Conc., Varian) equipped with 1 cm absorbance cells (Borosil). Multiplication of this value by a factor of 14.59 (Langlais et al. 1991) gives the ozone concentration in mg/L.

5.2.4 Cyanide Measurement

Free cyanide was measured by the titrimetric procedure using p-dimethyl- amino benzal-rhodanine as the indicator and $AgNO_3$ as titrant, as described in standard methods (Method No. 4500-CN^--D, APHA et al. 1995).

In solutions containing copper-cyanide complexes, EDTA was added for chelating copper from cyanide (Frant et al. 1972). The free cyanide was then estimated as per the cyanide electrode method (Method No. 4500-CN^-F, APHA et al. 1995) using a silver ion electrode (Orion No. 94-16, USA) used in conjunction with a single junction reference electrode (Orion No. KY1, USA), connected to digital ion analyzer (Systronics 2918, India).

5.2.5 Alkalinity Determination

Alkalinity was determined by the titrimetric method using methyl orange indicator (Method No. 2320 B, APHA et al., 1995).

5.2.6 pH Determination

pH was measured using a combination pH electrode (Toshniwal CL-51, India) connected to a digital pH meter (Toshniwal CL-54, India).

5.2.7 Nitrate Measurement

Nitrate was measured using an ion chromatograph (Metrohm 761) equipped with a Phenomenex STAR ION A 300 IC anion column, and conductivity detector with ion suppression. The method used (Method No. 2.6.3) for this purpose was specified in the relevant company literature (Metrohm, 1996).

5.2.8 Ammonia Measurement

Ammonia nitrogen was measured colorimetrically by Nesslerization (Method No. 417 B, APHA, et al., 1985). A spectophotometer (Spectronic, 20 D^+, India) with Borosil glass absorbance cells having 1cm path length were used for this purpose.

5.2.9 Cyanate Measurement

Cyanate was measured colorimetrically using Method No. 4500-CN^-L (APHA et al., 1995). A spectophotometer (Systronics, 100, India) with Borosil glass absorbance cells having 1cm path length were used for this purpose.

5.3 Experimental Setup

The experimental setup consisted of a continuous-flow counter-current bubble contactor as shown in Figure 4.1. Samples could be extracted from the reactor by using a syringe connected to the sampling port of the reactor, as shown in the same figure. Ozone was generated in gas phase by passing pure oxygen from an oxygen cylinder through an ozone generator (INDIZONE, CDS/4C/AF, India). Arrangements were made for applying this gas mixture containing ~1 percent ozone to the bottom of the reactor, where it bubbled through a porous ceramic plate and moved upwards through the reactor. The gas flow into the reactor was controlled using an on-line mass flow controller (AALBORG, GFC171S, USA). The ozone concentration in the gas influent to the reactor was measured using an online ozone monitor (ANSEROS, Ozomat GM-6000-OEM). Arrangements were also made for measuring the ozone concentration in the gas effluent from the reactor. The liquid phase was introduced into the reactor from the top using a multi-channel peristaltic pump (IKA PA-MCP). Liquid was also extracted at the same rate from the bottom of the reactor using the same pump, thus maintaining a

continuous liquid flow in the reactor. All components of the experimental setup and the reactor were made of glass, teflon or stainless steel to ensure that ozone consumption due to corrosion of components by ozone leading the erroneous experimental results is fully eliminated. A schematic of the experimental setup is shown in Figure 5.1.

5.4 Description of Experiments Conducted

5.4.1 Experiment Type I: Ozonation of Pure Water

Triple distilled water was pre-ozonated to ensure that both inorganic and organic impurities were minimized to the extent possible. The pH and C_T of this water was then adjusted to the desired value by addition of the desired amounts of $NaHCO_3$ / Na_2CO_3 and HCl / NaOH. Approximately three liters of water purified and prepared as above was required for each experiment.

The valves in the experimental setup were set as in case I, Figure 5.1, and oxygen flow at the desired rate was started through the reactor by adjusting the MFC appropriately. The influent ozone concentration, as measured by the online ozone monitor was zero at this time. The reactor was filled up with liquid prepared as above employing the peristaltic pump in the 'fast' mode. Next, a continuous liquid flow at the desired rate was established through the reactor employing the peristaltic pump appropriately. Care was taken to ensure at this point that both gas and liquid flow rates through the reactor were steady and of the value desired.

Next, the ozonator was turned on. This resulted in the increase of gaseous ozone concentration, as determined by the ozone monitor, from zero to an increased, but constant value. This gaseous ozone concentration was recorded as the influent gaseous ozone concentration to the reactor. Next the valve of the experimental setup were adjusted as in case II, Figure 5.2, in order to measure the effluent ozone concentration from the reactor. Attainment of constant gaseous ozone concentration in the effluent side was taken as an indication that 'steady-state' has been attained in the reactor. Next, five aliquots of 5 ml. each were taken at five-minute intervals from the reactor for the measurement of aqueous ozone concentration in the reactor using the Indigo method.

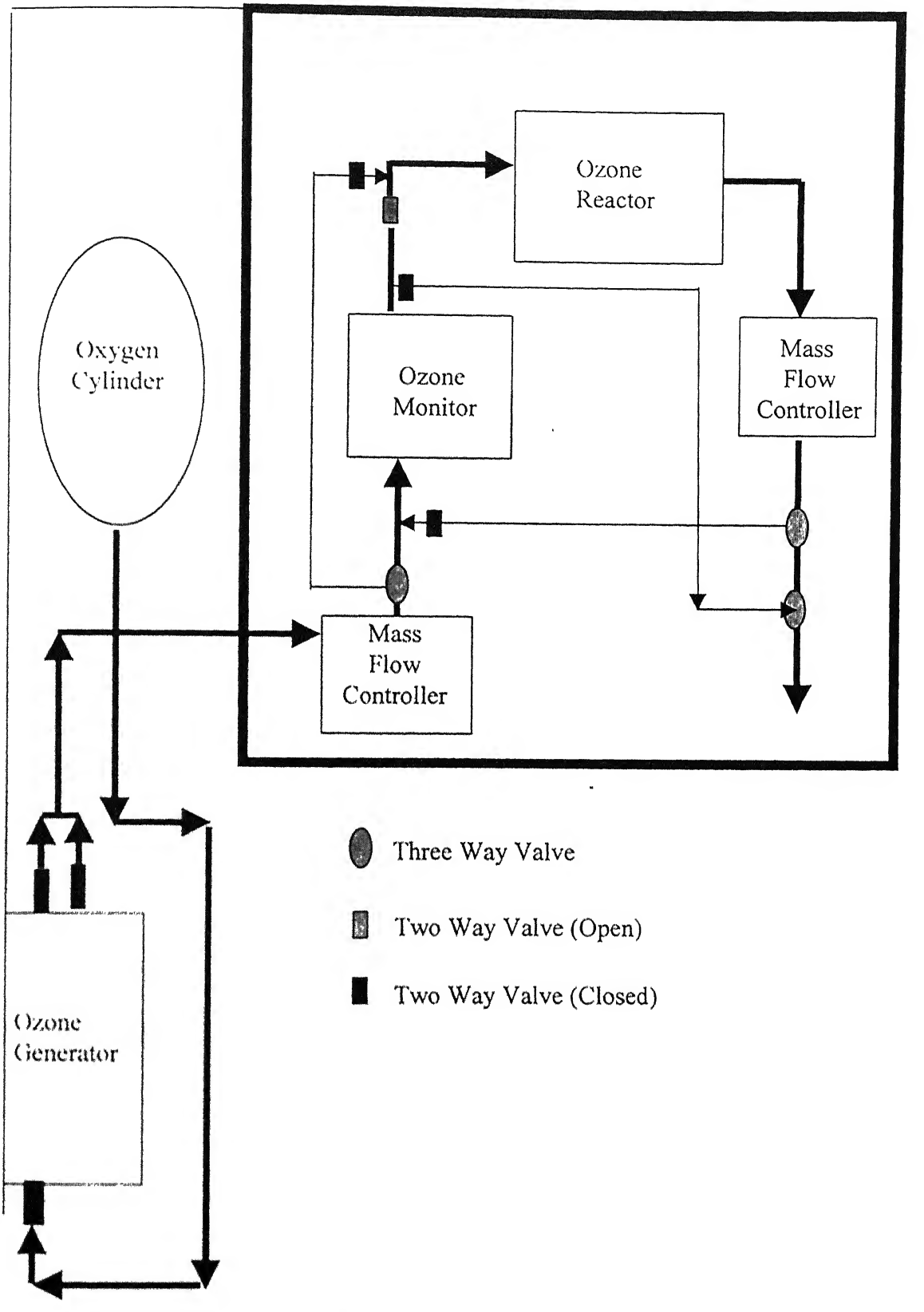

Figure 5.1 Schematic of Experimental Set-up
Case A. Measuring Influent Gaseous Ozone Concentration

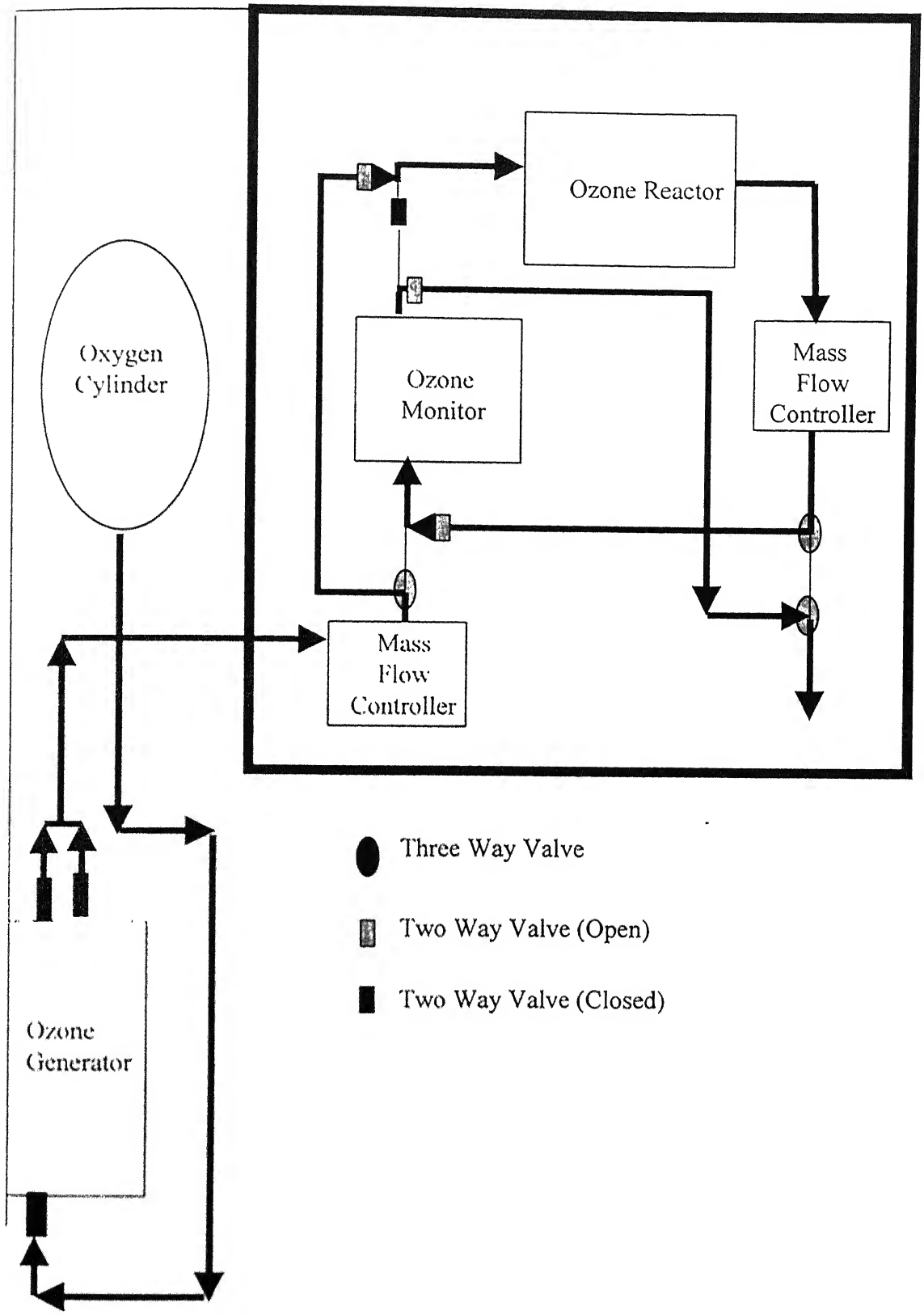

Figure 5.2 Schematic of Experimental Set-up
Case B. Measuring Effluent Gaseous Ozone Concentration

5.4.2 Experiment Type II: Ozonation of Water Containing Free and Complexed Cyanide

Pre-ozonated triple distilled water was prepared as described in the previous section. The pH and C_T of this water was then adjusted to the desired value by addition of the desired amounts of Na_2CO_3 and NaOH. Required amounts of KCN or KCN/CuCN stock solution was added such that the concentration of free or complexed cyanide in the water was as desired.

After attaining constant gas and liquid flow in the reactor, as described in the previous section, the ozonator was turned on. Five aliquots of 10 mL each were extracted from the reactor at 0, 5, 10, 15, 20 minutes for experiments with free cyanide. Five aliquots of 10 mL each were extracted at 0, 25, 30, 35 and 40 minutes for experiments with complexed cyanide. Each aliquot was analyzed for residual cyanide and probable ozonation by-products like cyanate, ammonia and nitrate. Influent and effluent gaseous ozone concentration was also noted during all the experiments.

CHAPTER VI

RESULTS AND DISCUSSION: EXPERIMENTAL VALIDATION OF THE MATHEMATICAL SIMULATION OF OZONE MASS TRANSFER AND DECOMPOSITION IN PURE WATER

6.1 Introduction

A model for mathematical simulation of ozone mass transfer and decomposition in pure water in a continuous counter flow bubble contactor was developed in Chapter IV. The model inputs were the reactor dimensions, gas flow rate (Q_g), liquid flow rate (Q_l), influent gaseous ozone concentration, $[O_3]_g^i$, water pH, aqueous scavenger concentration (C_T), mass transfer coefficient ($K_L.a$) and the solubility ratio (S). The last two variables are temperature dependent, and hence temperature is also an implicit input variable to the model. Also, 'S' is a function of Henry's constant, $H_{[O_3]}$, for ozone equilibrium between gas and liquid phases. Given the above inputs, the model is able to calculate the steady-state concentrations of all relevant species in both gaseous and liquid phases participating in ozone mass transfer and decomposition processes. In this chapter, experimental validation of the above model is provided through comparison of experimentally derived data on effluent gaseous ozone concentration and aqueous ozone concentration obtained under a variety of conditions with corresponding values obtained from the model simulation.

6.2 Analysis of Reactor Characteristics

The configuration and dimensions of the reactor used for the simulation studies described previously and the experimental studies to be discussed hence is described in section 4.2. While discussing the reactor characteristics it was mentioned that the reactor contents are assumed to be completely mixed, both in liquid and gaseous phases. This enables one to assume that under steady-state conditions, the concentration of all species in the aqueous and gaseous phase inside the reactor is constant both with respect to time and position, and is equal to the concentration of these species effluent from the reactor.

In order to determine the validity of the assumption that the liquid phase in the reactor is completely mixed, tracer studies were performed at two different liquid flow rates (Q_l) of 25 mL/min and 10 mL/min. The gas flow (Q_g) rate during the above studies was maintained constant at 1 L/min. A typical experiment consisted of achieving steady gas (oxygen) and liquid (water) flow through the reactor as per conditions mentioned above. Next, a slug of dye was introduced into the reactor, and the absorbance due to effluent dye concentration was measured over time. Results of such measurement are shown in Figures 6.1a and 6.1b. The performance of an ideal completely mixed reactor operating under the same conditions was calculated, and is shown in the same figures for comparison purposes. Visual comparison of the results indicated that the reactor was very nearly a CSTR. However, no further mathematical calculations were performed to validate this point.

Validity of the assumption that the gas-phase in the reactor is completely mixed is more difficult to prove. No experiments could be performed to verify this assumption. Literature review (e.g., Nishikawa et al., 1981) on this subject indicated that there is some dispute on whether the gas phase should be described as completely mixed or plug flow. Though a majority of researchers have modeled the gas phase in such reactors as completely mixed (e.g., Anselmi et al., 1984; Roustan et al., 1087), others (Wu and Masten, 2001) have used both kinds of flow regime and concluded the plug flow model to be superior. However, for the model described in this dissertation, the gas phase in the reactor was considered to be completely mixed, based on the assumption that in reactors with low length to diameter ratio (4.81 in this case), a choice either one way or the other makes little or no difference.

6.3 Experimental Determination of $K_L.a$

Experimental determination of $K_L.a$ for the reactor under question was performed to obtain a validation for the theoretically calculated $K_L.a$ values used for simulation in Chapter IV. Experiments were performed at two different liquid flow rates (Q_l) of 25 mL/min and 10 mL/min for this purpose. The gas flow (Q_g) rate during the above studies was maintained constant at 1 L/min. A typical experiment was conducted with pure

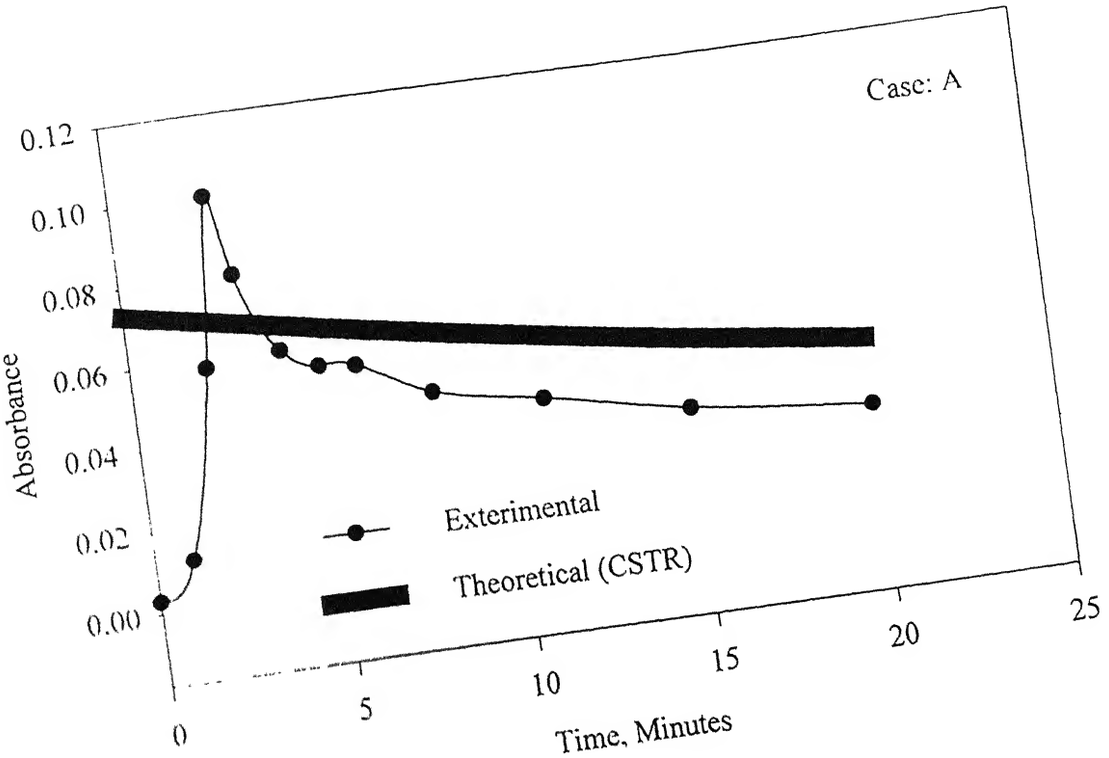

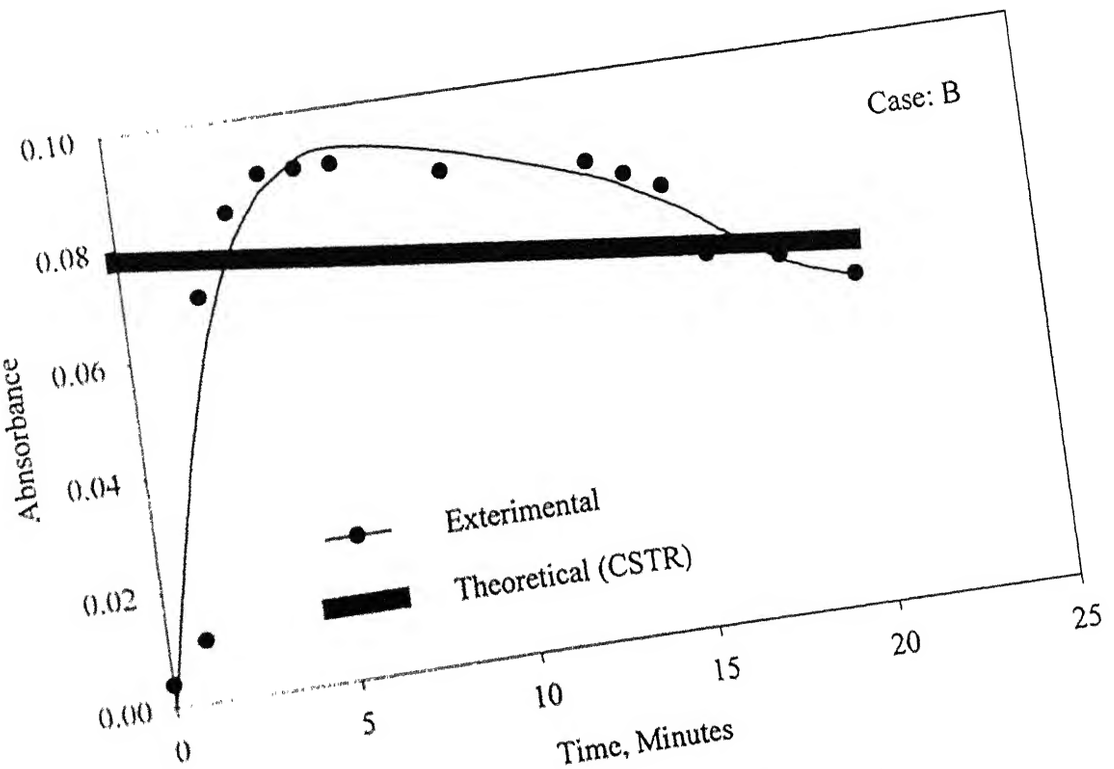

Figure 6.1. Reactor Response to Slug Input (V = 1 L)
A. Q_i = 25 mL/min; B. Q_i = 10 mL/min

water at high pH (~12) and no added scavenger (C_T), and consisted of achieving steady gas (oxygen) and liquid (water) flow through the reactor as per conditions mentioned above. Next, the ozonator was started such that gaseous ozone was influent to the reactor. Sufficient time was provided for the system to attain 'steady-state' under these conditions. Next the influent gaseous ozone concentration, $[O_3]_g^i$, the effluent gaseous ozone concentration, $[O_3]_g$, and the aqueous ozone concentration, $[O_3]$, in the reactor was measured. Based on these values, $K_L.a$ of the reactor could be calculated as below.

Mass transfer of ozone from the gaseous to the liquid phase can be represented the Equation 6.1,

$$Q_g\left\{[O_3]_g^i - [O_3]_g\right\} = V.(K_L.a)\left\{[O_3]_l^s - [O_3]_l\right\} \qquad \text{Equation 6.1}$$

Where,

Q_g = Gas Flow Rate, L/min

$[O_3]_g^i$ = Influent Gaseous Ozone Concentration, mg/L

$[O_3]_g$ = Effluent Gaseous Ozone Concentration, mg/L

V = Reactor Volume, L

$K_L.a$ = Mass Transfer Coefficient, /min

$[O_3]_l^s$ = Saturation Ozone Concentration in aqueous phase, mg/L = $S.[O_3]_g$

$[O_3]_l$ = Aqueous Ozone Concentration, mg/L

When pure water is ozonated, and the pH of the aqueous phase is 12, aqueous ozone concentration, $[O_3]_l$, is negligibly small. The above assumption was verified by measuring aqueous ozone concentration, as stated above. Hence the term $[O_3]_l$ in Equation 6.1 may be neglected in comparison to other terms in the equation. Thus $K_L.a$ may be represented as,

$$K_L.a = \frac{Q_g\left\{[O_3]_g^i - [O_3]_g\right\}}{V.[O_3]_l^s} = \frac{Q_g\left\{[O_3]_g^i - [O_3]_g\right\}}{V.S.[O_3]_g} \qquad \text{Equation 6.2}$$

The value of 'S' in the above expression may be calculated as shown in section 4.3.2. Since all other quantities in the right side of Equation 6.2 are known, the value of $K_L.a$ could be calculated.

The value of $K_L.a$ calculated in the above fashion was $0.48\pm0.04\ s^{-1}$ for Q_l of 25 mL/min and $0.48\pm0.03\ s^{-1}$ for Q_l of 10 mL/min. The temperature during the above experiment was 35°C. These values are in approximate agreement with the theoretically calculated $K_L.a$ value of ~$0.4\ s^{-1}$ at 30°C, as shown in Table 4.5.

6.4 Experimental Condition for Ozonation Studies

Experimental ozonation studies were conducted under a variety of conditions are shown in Table 6.1. The variables monitored during experiments were $[O_3]_g$, and $[O_3]_l$. The gas flow rate (Q_g) and liquid flow (Q_l) rate values were held constant at 1 L/min and 25 mL/min respectively. Parameters that were varied included solution pH, scavenger concentration (C_T) and influent gaseous ozone concentration ($[O_3]_g^i$). For each experiment, sufficient time was allowed to elapse after the start of ozonation before readings/samples were take to ensure the attainment of 'steady-state'. Generally for each experiment, five readings/samples were taken at five-minute intervals. The average and standard deviation of these values have been presented in Table 6.1. In all a total of 34 experiments of this type were performed.

6.5 Comparison of Experimental Results with Mathematical Simulation

For the purpose of comparison of experimental data with modeling results, simulations were run using the model developed in Chapter IV under each of the experimental conditions as shown in Table 6.1. Next, the experimental result and the value obtained under same conditions through simulation were plotted against each other. This procedure was followed for all 34 conditions, under which experimental results were obtained. Graphs of this type were drawn for both aqueous ozone concentration in the reactor and effluent gaseous ozone concentration from the reactor.

Table 6.1 Summary of Experimental Conditions and Experimental Results Concerning Ozonation of Pure Water

Expt. No.	pH	Scavenger C_T, mM	Influent Gaseous Ozone, $[O_3]_g^i$, mg/L	Effluent Gaseous Ozone $[O_3]_g$, mg/L		Aqueous Ozone $[O_3]_l$, mg/L	
				Average	Standard Deviation	Average	Standard Deviation
1.	8.80	1.00	35.50	32.20	0.76	2.88	0.29
2.	8.80	1.00	26.00	21.34	0.89	2.28	0.27
3.	8.80	1.00	28.00	24.60	1.61	2.42	0.25
4.	8.80	1.00	50.00	43.94	2.88	4.70	0.13
5.	8.80	1.00	38.00	32.04	1.73	3.47	0.60
6.	8.80	1.80	27.00	21.44	1.95	2.08	0.30
7.	8.80	5.00	36.00	33.48	0.43	3.55	0.28
8.	8.80	5.00	26.00	23.34	1.46	2.59	0.14
9.	8.80	5.00	24.00	21.44	1.57	2.35	0.14
10.	8.80	5.00	50.00	44.54	1.89	6.07	0.38
11.	8.80	5.00	34.00	33.06	1.45	3.03	0.58
12.	8.80	10.00	36.00	34.18	0.75	4.26	0.50
13.	8.80	10.00	27.00	24.32	0.72	2.91	0.23
14.	8.80	10.00	26.00	24.20	1.92	2.52	0.55
15.	8.80	10.00	50.00	47.18	1.56	6.68	0.24
16.	8.80	10.00	36.00	34.68	1.21	2.73	0.67
17.	8.80	10.00	28.00	24.02	0.80	3.84	0.32
18.	8.80	100.00	26.00	25.10	0.43	3.71	0.30
19.	3.00	0.00	35.50	35.04	0.77	6.19	0.43
20.	3.00	0.00	26.50	26.10	0.59	5.79	0.39
21.	3.00	0.00	28.00	26.10	2.30	4.89	0.39
22.	3.00	0.00	48.50	47.86	1.25	7.79	0.41
23.	7.00	1.00	35.00	33.22	0.75	3.58	0.32
24.	7.00	1.00	27.00	25.34	0.44	3.09	0.49
25.	7.00	1.00	25.00	22.84	2.60	2.42	0.56
26.	7.00	1.50	31.00	26.98	1.83	4.75	0.22
27.	7.00	5.00	35.00	34.16	0.38	4.34	0.18
28.	7.00	5.00	26.00	25.64	0.43	4.01	0.52
29.	7.00	5.00	25.00	23.84	1.94	2.88	0.43
30.	7.00	10.00	35.00	34.32	0.75	4.55	0.35
31.	7.00	10.00	28.00	26.70	0.42	4.13	0.39
32.	7.00	10.00	30.00	29.14	0.75	5.14	0.32
33.	7.00	10.00	25.50	24.66	2.91	3.74	0.62
34.	7.00	100.00	30.00	29.40	0.75	5.26	0.32

6.5.1 Aqueous Ozone Concentration

Comparison of measured and simulated aqueous ozone concentration in the reactor for experimental conditions presented in Table 6.1 are plotted in Figure 6.2. A line of unit slope is also drawn in the same figure, a point lying on this line suggesting perfect agreement between experimental and simulation results. A point below this line suggests under-simulation of the experimental value, while a point above this line suggests over-simulation. A regression line is also drawn in the same figure to indicate degree of agreement between experimental and simulated value. The correlation coefficient between the experimental and simulated values in this case was found to be 0.544. The reasons for the relatively low value of the correlation coefficient will be discussed in section 6.6.

6.5.2 Effluent Gaseous Ozone Concentration

Similar comparison as above for gaseous ozone concentration effluent from the reactor is shown in Figure 6.3. For a majority of experiments in this case, a very good agreement between experimental and corresponding simulated result is noticed. However, severe under-prediction by the model of some experimental result results in relatively moderate correlation coefficient of 0.539 in this case also. The reasons for such under prediction will be discussed in section 6.6.

6.6 Discussion of Results

Based on the results presented in Figures 6.2 and 6.3 it may be concluded that the agreement between experimental data and simulation results is only moderate. The reported correlation coefficients in the above figures could have been enhanced significantly if some poorly correlating data points were omitted as possible 'outliers'. However, that would have defeated the objectives of the discussion in this section, which is geared towards exploring the reasons behind disagreement between some of the experimental data with simulation results.

To begin such a discussion, one must first look at some of the deficiencies of the simulation model developed in Chapter IV, and the possible impacts of these deficiencies

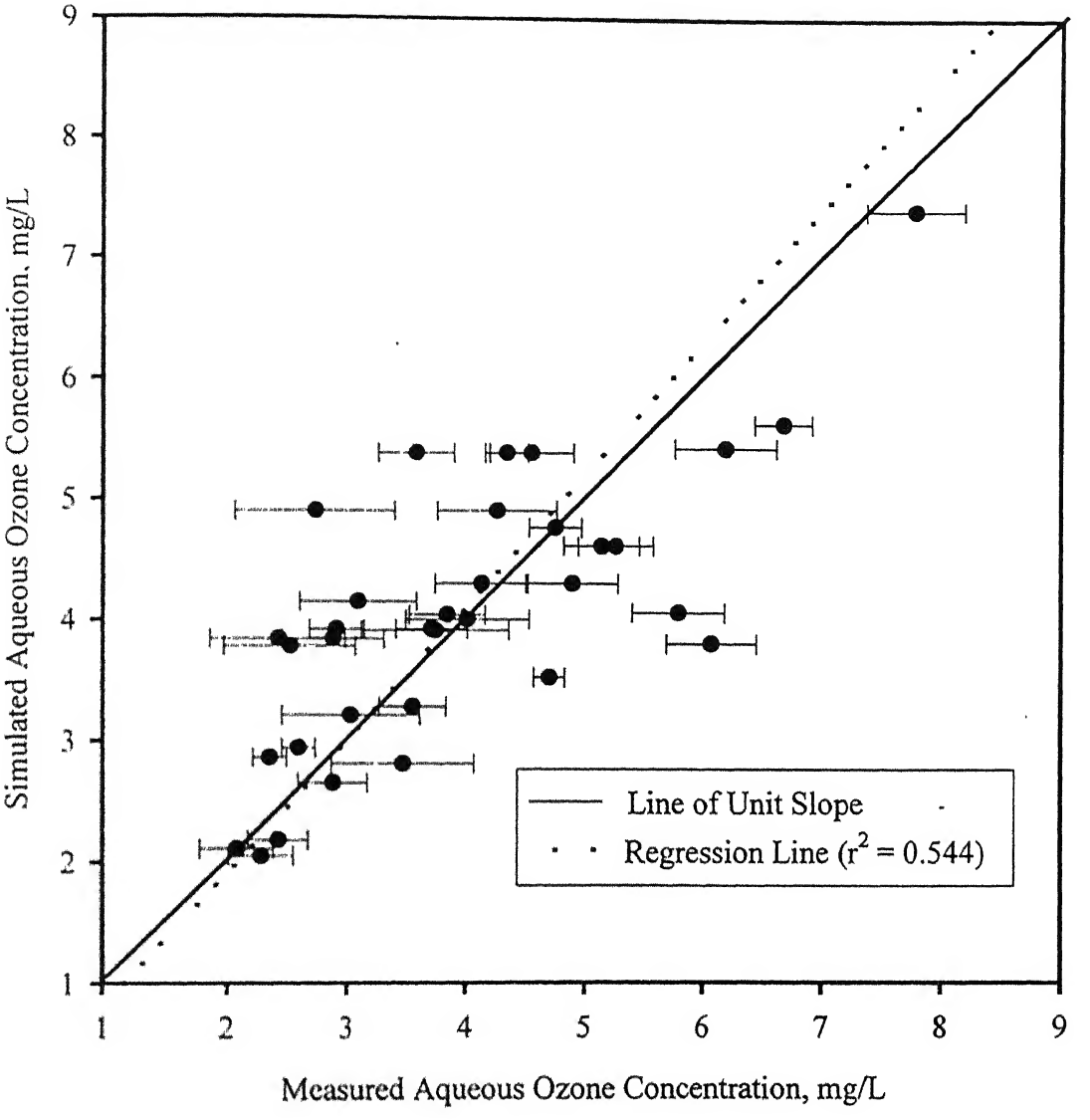

Figure 6.2 Comparison of Measured and Simulated Aqueous Ozone Concentration for Experimental Conditions Given in Table 6.1
(Q_l = 25 mL/min; Q_g = 1 L/min; Temperature = 30±3 °C)
(Error Bars are Based on Standard Deviation of Measured Values)

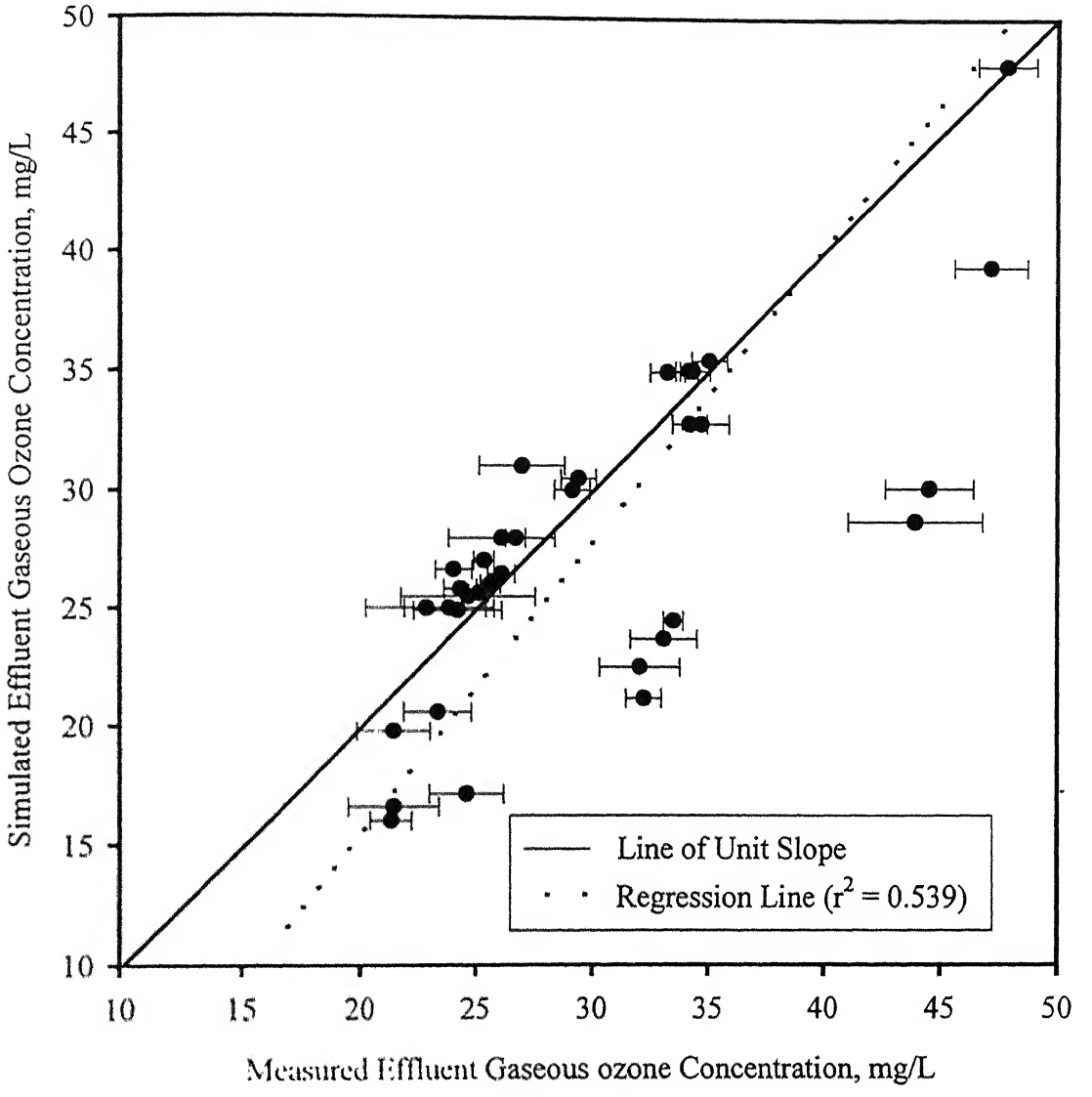

Figure 6.3 Comparison of Measured and Simulated Effluent Gaseous Ozone Concentration for Experimental Conditions Given in Table 6.1
(Q_l = 25 mL/min; Q_g = 1 L/min; Temperature = 30±3 °C)
(Error Bars are Based on Standard Deviation of Measured Values)

on the simulation results. One assumption made while formulating the model was that the gas phase in the reactor was completely mixed. The effect of this assumption, if incorrect, would be to over-predict the effluent gaseous ozone concentration. However, results in Figure 6.3 indicate that gaseous ozone concentration is under-predicted in many cases. Another assumption was that no ozone decomposition occurs in the gas phase. The net effect of invalidity of this assumption will also be over-prediction of the effluent gaseous ozone concentration. Further more, (Wu and Masten, 2001) indicated that as per their experimental observation, the steady-state ozone concentration at the entrance of and at the exit to the reactor headspace was unchanged corresponding to headspace detention time of up to 20 minutes. The retention time of ozone in the headspace of the reactor described in this dissertation is less than 20 minutes.

It is postulated that differences in temperature and ionic strength values between the experimental and simulated results may account for most of the variability seen in Figures 6.2 and 6.3. It is well known that the mass transfer coefficient ($K_l.a$) increases with increase in temperature, while the solubility ratio (S) of ozone decreases with temperature. The solubility ratios (S) of ozone are reported to be 0.34, 0.24 and 0.17 for temperatures of 12°, 21° and 31°C respectively (Caprio et al., 1981), which are in good agreement with values calculated in Chapter IV of this dissertation. Furthermore, sensitivity analysis (Wu and Masten, 2001) showed that the solubility ratio (S) is the parameter that is most sensitive in determining the concentration of aqueous ozone and hence effluent gaseous ozone concentration from the reactor. Also, ionic strength and mass transfer coefficient is positively correlated. This is due to the reduction in the surface tension of water with increase in ionic strength (Cogo et al., 1999), which results in decrease in bubble size and corresponding increase in specific interfacial area (a), thus increasing the mass transfer coefficient ($K_l.a$). The solubility ratio (S) is however, not affected by the ionic strength of water. The experiments described in this dissertation were conducted at 30±3°C. This 6°C variation in temperature may explain the variation between experimental and simulation results. Simulation temperature was fixed at 30°C. Furthermore, the ionic strength was not controlled during these experiments. This may also lead to some variation between the experimental and simulated results.

CHAPTER VII

RESULTS AND DISCUSSION: OZONATION OF FREE AND COMPLEXED CYANIDE AND EVOLUTION OF BY-PRODUCTS

7.1 Introduction

The objective of the experiments described in this chapter is to study the rate and extent of degradation of free and copper-complexed cyanide by ozonation. Another objective is to monitor the evolution of the cyanide degradation by-products produced through ozonation. The reactor used for this study has been described and characterized in Chapters IV and V. Description of the experimental setup used and the experimental procedure are given in Chapter V.

7.2 Ozonation of Free Cyanide

On ozonation, free cyanide may either react with molecular ozone or with [•OH] radicals produced though decomposition of ozone in aqueous systems. Mathematically, the rate of cyanide destruction at high pH, where $CN^- >> HCN$, may be written as,

$$\text{Rate of Cyanide Destruction} = \frac{d[CN^-]}{dt} = K_{CN^-,O_3}[CN^-].[O_3] + K_{CN^-,\bullet OH}[CN^-].[\bullet OH] \qquad \text{Equation 7.1}$$

However at high pH the aqueous ozone concentration is expected to be low. Also based on the molecular structure of cyanide molecule, it is apparent that it is unlikely to react substantially with molecular ozone, i.e., K_{CN^-,O_3} is expected to be small. Considering the above points, it may be assumed that, $K_{CN^-,O_3}[CN^-].[O_3] << K_{CN^-,\bullet OH}[CN^-].[\bullet OH]$. Hence,

$$\text{Rate of Cyanide Destruction} = \frac{d[CN^-]}{dt} \approx K_{CN^-,\bullet OH}[CN^-].[\bullet OH] \qquad \text{Equation 7.2}$$

पुरुषोत्तम काशीनाथ केलकर पुस्तकालय
भारतीय प्रौद्योगिकी संस्थान कानपुर
141824
अवाप्ति क्र० A

7.2.1 Experimental Conditions

Experimental variables that affect the destruction of cyanide by ozonation are pH, scavenger concentration (C_T), influent gaseous ozone concentration ($[O_3]_g^i$), gas flow

rate (Q_g), liquid flow rate (Q_l) and influent cyanide concentration ($[CN^-]_i$). Of these variables, only three, i.e., C_T, Q_l and $[O_3]_g^i$ were varied during the course of the experiments described herein. Experimental conditions for conduction various experiments are presented in Table 7.1.

Table 7.1 Experimental Conditions for Ozonation of Free Cyanide

No.	pH	C_T, mM	$[O_3]_g^i$, mg/L	Q_g, L/min	Q_l, mL/min	$[CN^-]_i$, mg/L	Sampling Time, Minutes
A	12.8	3	40.30±0.73	1.0	25	112.14	0, 5, 10, 15, 20
B	12.8	1	40.90±1.35	1.0	25	103.74	0, 5, 10, 15, 20
C	12.8	2	40.06±0.42	1.0	25	100.28	0, 5, 10, 15, 20
D	12.8	3	39.42±2.57	1.0	30	101.27	0, 5, 10, 15, 20
E	12.8	3	40.30±1.20	1.0	10	110.32	0, 5, 10, 15, 20
F	12.8	3	35.10±0.80	1.0	25	108.68	0, 30, 40, 60, 90, 120

Experiments A, B and C are similar in all respects, except for the varying scavenger (C_T) concentration. Experiments D and E are similar to experiment A in all respects expect for differences in Q_l values. Experiment A and F is identical, except that influent ozone concentration, $[O_3]_g^i$ are different. Also, sampling was done at later times in case of experiments F, as compared to experiment A, in order to demonstrate the onset of steady-state conditions at after the passage of sufficient time from the start of the experiment.

7.2.2 Kinetics of Free Cyanide Degradation

It is expected that after the starting of ozonation, the effluent free cyanide concentration in the reactor will decline and stabilize at a constant or 'steady-state' value after some time. In order to determine the time required for attaining the steady state, a cyanide degradation experiment (Experiment F) was run for 120 minutes. Results of this experiment, as presented in Figure 7.1 indicate that 'steady-state' was reached within 30

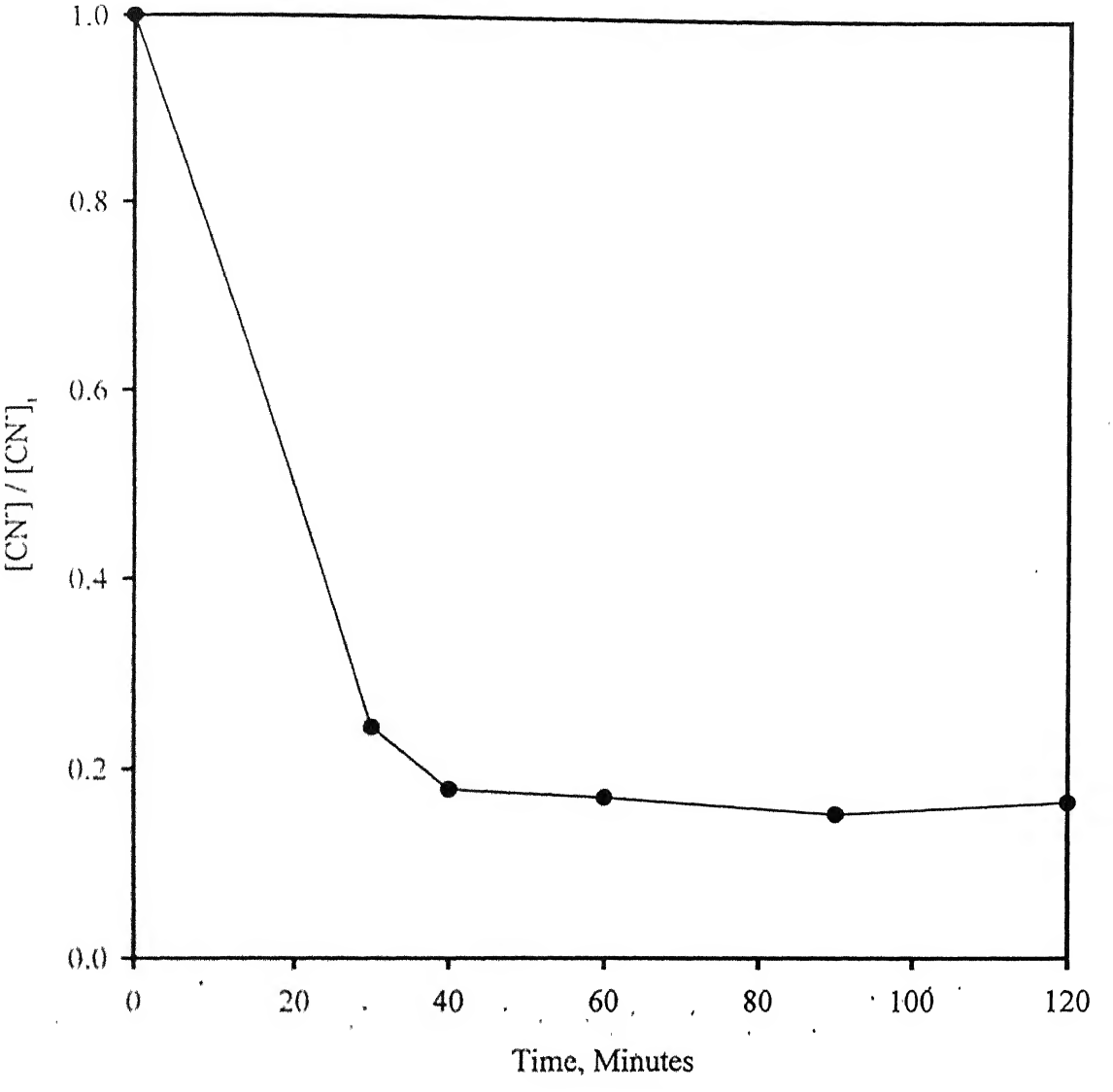

Figure 7.1 Attainment of Steady State During Free Cyanide Degradation by Ozonation ($[O_3]_g^1$: ~ 35 mg/L; $[CN]_i$ ~ 100 mg/L; Q_g = 1.0 L/min; Q_l = 25 mL/min; V = 1 L)

minutes of the start of ozonation. Consequently, other similar experiments were conducted for 30 minutes duration only.

Effect of scavenger concentration on the cyanide degradation rate by ozonation, as determined through Experiments A, B and C are shown in Figure 7.2. After the start of ozonation, the free cyanide concentration in the reactor shows a consistent decline in all three cases, with steady-state conditions being reached in 30 minutes. The observed rate of degradation is similar for cases with scavenger (C_T) concentrations of 3 and 2 mM (Experiments A and C), while the degradation rate in the 1 mM case (Experiment B) is decidedly more rapid. Nonetheless, it was also observed that the steady-state effluent cyanide concentration observed in all three cases were essentially similar, with steady-state removal percentage of between 90 and 95 percent.

These results are explicable in terms of the understanding of the effect of scavenger concentration on ozone decomposition. Enhanced scavenger concentration results in the hindrance of promotion reactions and hence slows down ozone decomposition, resulting in maintenance of lower [•OH] radical concentration in the reactor. Since rate of cyanide destruction is directly proportional to the [•OH] radical concentration in the reactor, a higher scavenger concentration should result in less cyanide destruction and hence higher cyanide concentration in the effluent from the reactor.

The influence of liquid throughput on the cyanide degradation rate by ozonation, as determined through experiments A, D and E are shown in Figure 7.3. The observed rate of degradation is slowest when the liquid throughput was 30 mL/min (Experiment D). The observed rate of degradation was the fastest when the liquid throughput was decreased to 10 mL/min (Experiment E). In the last case (Experiment E), the cyanide concentration declined to below detection levels within 5 minutes of the commencement of ozonation. Moreover, the 'steady-state' cyanide removal percentages also varied with the liquid throughput, with these values being 83, 91 and 100 percent for liquid flow-rates of 30, 25 and 10 mL/min.

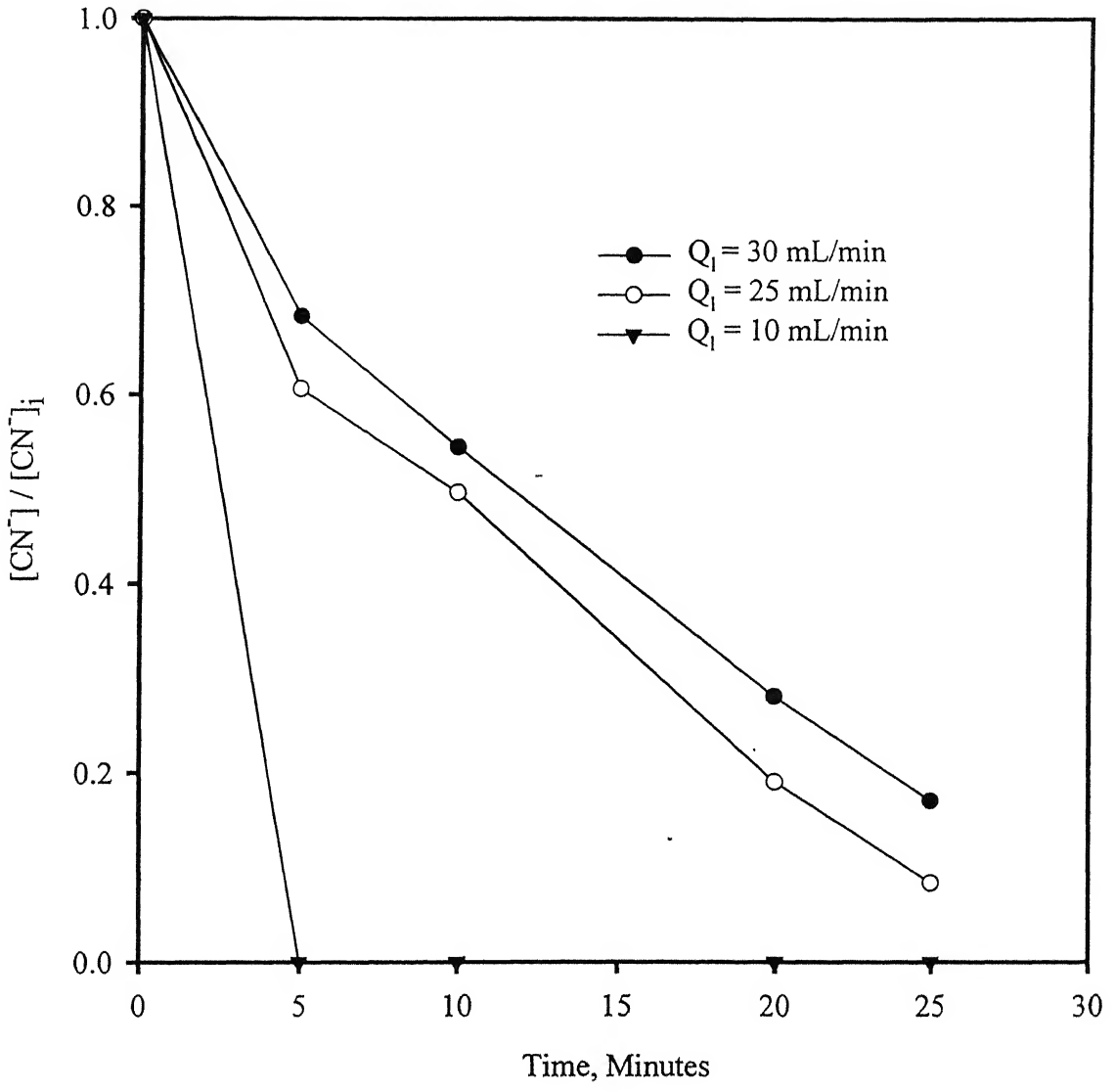

Figure 7.3 Effect of Liquid Flow rate (Q_l) on Free Cyanide Degradation by Ozonation ($[O_3]_g^i$: ~ 40 mg/L; $[CN^-]_i$ ~ 100 mg/L; Q_g = 1.0 L/min; C_T = 3 mM)

7.2.3 Evolution of By-Products

By products formed due to the ozonation of cyanide are generally assumed to be inorganic nitrogen-containing compounds like cyanate (CNO^-), ammonia (NH_3) and nitrate (NO_3^-). For the purpose of monitoring the evolution of by-products of ozonation of cyanide, samples collected during experiments A-F were screened for the above compounds in addition to residual free cyanide. Concentrations of all compounds measured were expressed in terms of nitrogen, and nitrogen balance of the constituents performed. Results are presented in terms of these nitrogen balances performed for each sample.

Nitrogen balance performed for various samples collected during experiment F are presented in Figure 7.4. As per results presented in this figure, the main by-product of cyanide oxidation by ozonation is cyanate (CNO^-). Other by-products of ozonation that were identified and measured included ammonia (NH_3) and nitrate (NO_3^-), which are present in much lower concentration than cyanate (CNO^-), and are thought to be formed due to sequential degradation of cyanate (CNO^-) to ammonia (NH_3) and nitrate (NO_3^-). Mass balance results show total recoveries of 90 percent or more for each of the samples tested. Thus it may be concluded that all the important by-products of cyanide oxidation have been identified and monitored in the course of this analysis. Similar mass balances for the other experiments performed are presented in Figure 7.5 (Experiments A, B and C) and Figure 7.6 (Experiments A, D, E). In all cases, cyanate (CNO^-) is found to be the major by-product of cyanide oxidation by ozonation. Additionally, cyanate (CNO^-) is further oxidized slowly to ammonia (NH_3) and then to nitrate (NO_3^-). However, the slowness of such oxidation is the reason for its persistence in solution.

The above hypothesis is supported by the perusal of the reported reaction rates (RCDC, 2002) of the above compounds with [$\bullet OH$]. These values are, $K_{CN^-,\bullet OH} = 8 \times 10^9$ L-

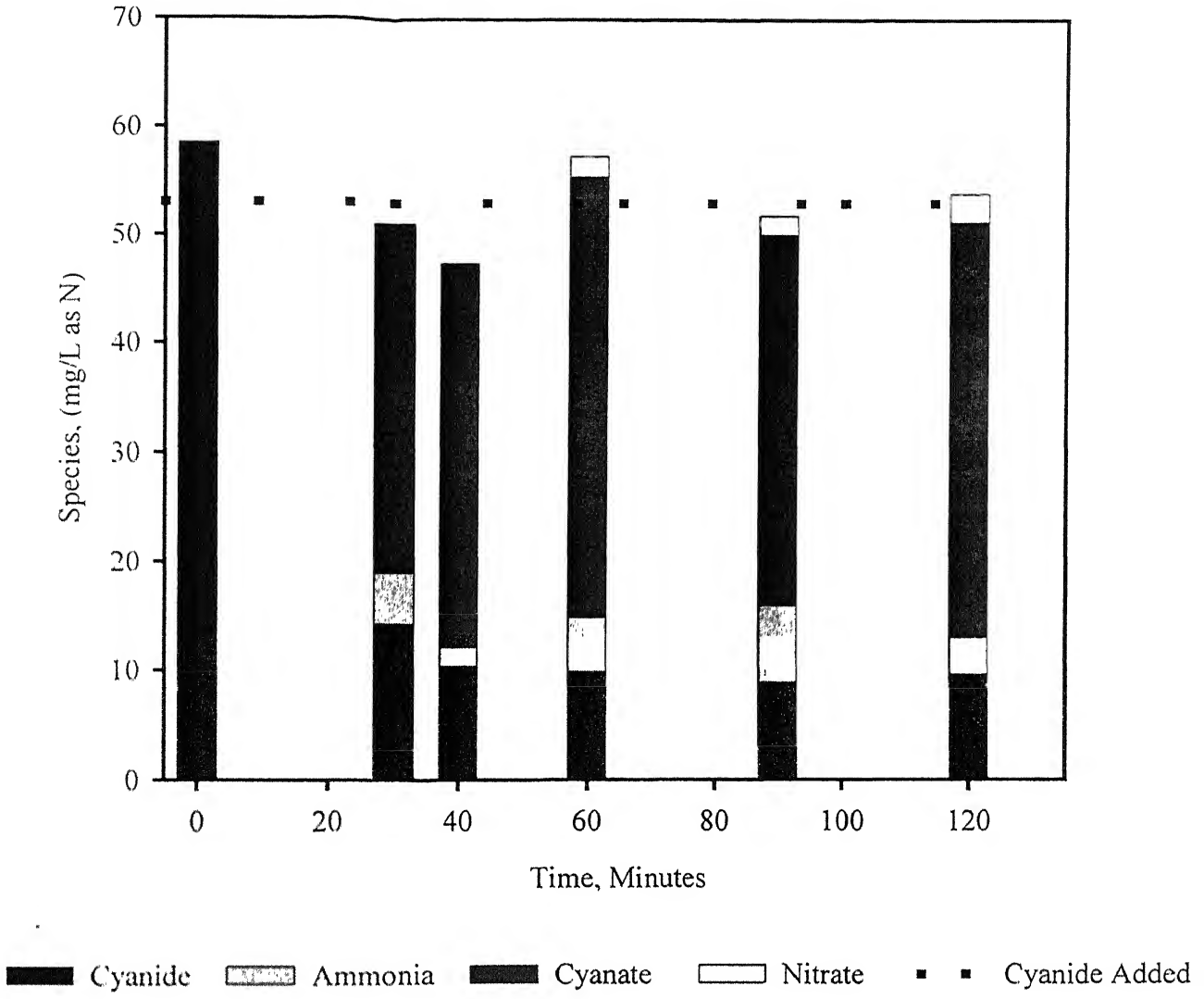

Figure 7.4 Evolution of By-Products Due to Degradation of Cyanide by Ozonation (Q_l = 25 mL/min; Q_g = 1 L/min, V = 1 L; $[O_3]_g^i \sim 35$ mg/L; C_T = 3 mM)

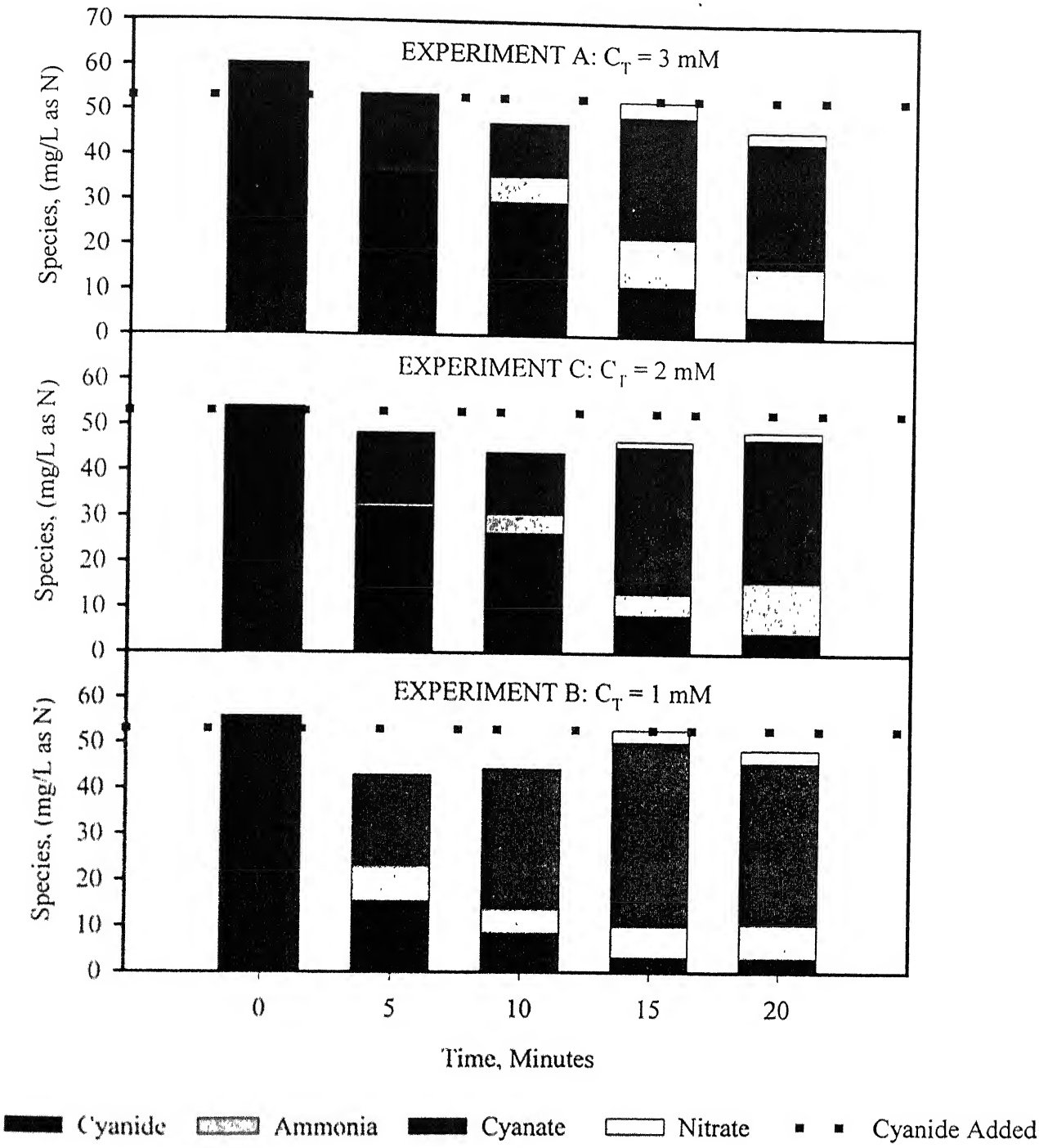

Figure 7.5 Effect of Scavenger Concentration (C_T) on Evolution of By-Products Due to Degradation of Free Cyanide by Ozonation
(Q_l = 25 mL/min; Q_g = 1 L/min; V = 1 L; $[O_3]_g^i \sim 40$ mg/L)

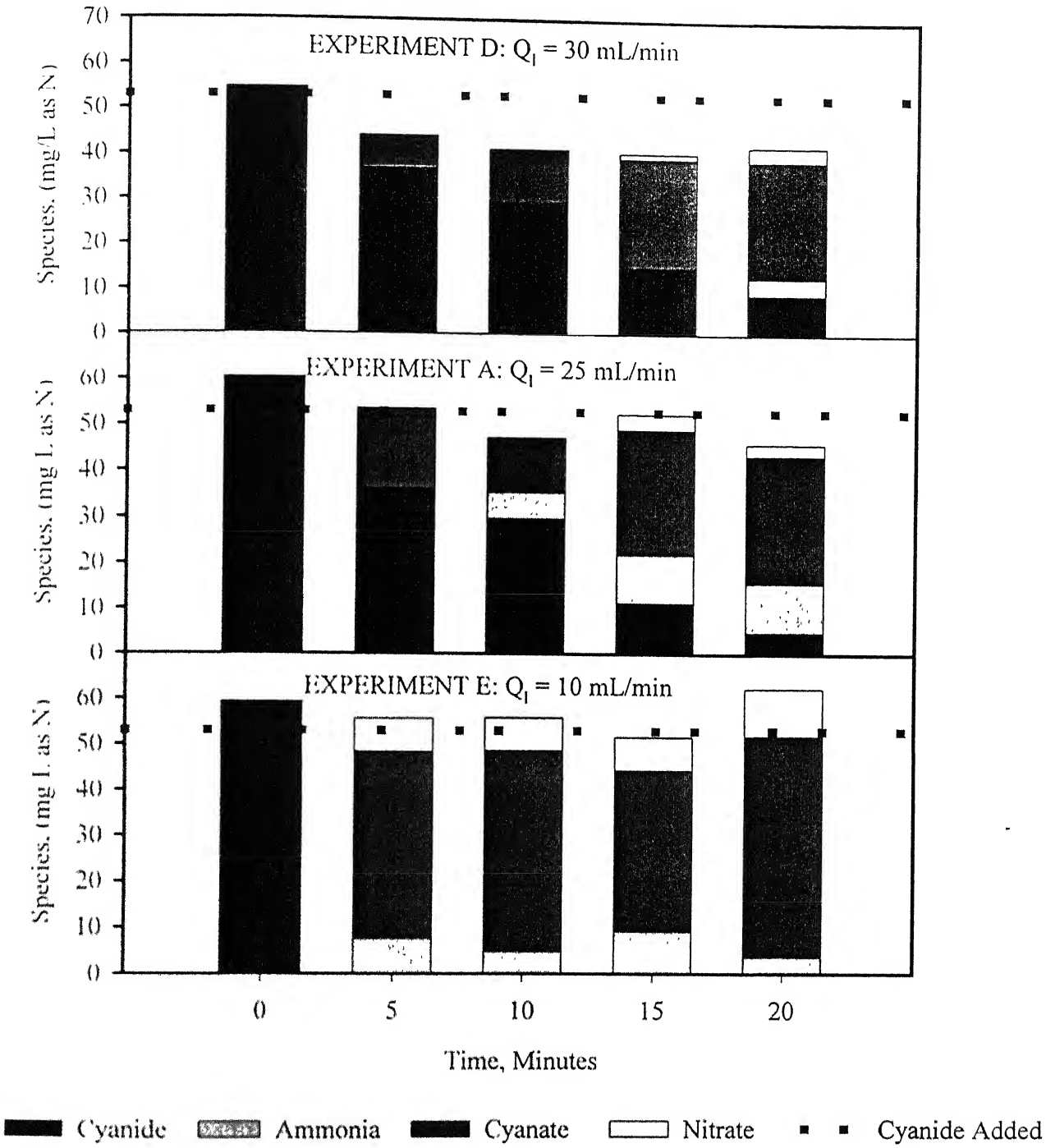

Figure 7.6 Effect of Liquid Flow Rate (Q_l) on Evolution of By-Products Due to Degradation of Free Cyanide by Ozonation
($C_{f_{CN}}$ = 3 mM; Q_g = 1 L/min; V = 1 L; $[O3]_g$: ~ 40 mg/L)

$mol^{-1}s^{-1}$, $K_{CNO^-,\bullet OH}$ =4.8 x 10^7 L-$mol^{-1}s^{-1}$ and $K_{NH_3,\bullet OH}$ =9.7 x 10^7 L-$mol^{-1}s^{-1}$, which clearly indicate cyanide oxidation to be nearly two orders of magnitude faster than the reaction of the degradation by-products like cyanate (CNO^-) and ammonia (NH_3) with hydroxyl radicals.

7.3 Ozonation of Copper-Complexed Cyanide

As in case of free cyanide, copper-complexed cyanide is also expected to interact [•OH] radicals produced though decomposition of ozone in aqueous systems. However, the rate of extent of such interaction is dependent on the affinity of [•OH] radicals towards cyanide, vis-à-vis the complexing agent. Thus in case of relatively weak complexers of cyanide such as zinc, complexation is expected to have little or no effect on cyanide degradation by ozonation. In case of stronger complexing agents of cyanide such as copper, the rate of cyanide degradation by ozonation may be hindered due to the presence of the complexing agent. In the presence of very strong cyanide complexing metals like iron, ozonation may be only marginally effective in effecting cyanide degradation.

Experiments described in the sections that follow were conducted with copper-cyanide complexes, which is an environmentally significant cyanide-complex due to its widespread use in metal-plating industry. It is expected that on ozonation, copper cyanide complexes will degrade, with cyanide decomposition resulting in the formation of by-products similar to those in case of free cyanide. Copper, which is present in the mono-valent state in such complexes, is expected to be oxidized to the cupric form and precipitate as $Cu(OH)_2$ or $CuCO_3$ or both, as per prevailing chemical conditions.

7.3.1 Experimental Conditions

Experimental variables affecting cyanide degradation were same in this case as for oxidation of free cyanide described earlier. However, only two variables, i.e., C_T, and Q_l, were varied during the course of the experiments described herein. Experimental conditions for conduction various experiments are presented in Table 7.2. Experiments G

and H is similar in all respects, except for the varying scavenger (C_T) concentration. Experiment I is similar to Experiment G, except for differences in Q_l values.

Table 7.2 Experimental Conditions for Ozonation of Complexed Cyanide

Sl. No.	pH	C_T, mM	$[O_3]_g^i$, mg/L	Q_g, L/min	Q_l, mL/min	$[CN^-]_i$, mg/L	Sampling Time, Minutes
G	12.5	3	39.56±1.65	1.0	25	95.0	0, 30, 40, 60, 90
H	12.5	1	39.56±1.82	1.0	25	105.0	0, 30, 40, 60, 90
I	12.5	3	39.44±1.44	1.0	10	105.0	0, 30, 40, 60, 90

7.3.2 Kinetics of Complexed Cyanide Degradation

As in case of experiments with free cyanide, after the start of ozonation, the cyanide concentration in the reactors with copper-complexed cyanide declined and stabilized at a steady value after some time for all three experiments. Effect of scavenger concentration on the cyanide degradation rate by ozonation, as determined through experiments G and H are presented in Figure 7.7. As seen from the results presented in this figure, 'steady-state' was reached in both cases within 30 minutes of the start of ozonation. However, the steady state cyanide concentration was lower for Experiment H (C_T = 1 mM, Cyanide Removal = 86 percent), as compared to experiment G (C_T = 3 mM, Cyanide Removal = 79 percent). Reasons for such behavior has been explained previously when discussing similar results concerning free cyanide. Additionally, the observed 'steady-state' effluent concentration in these cases were higher than corresponding steady-state concentration obtained under similar conditions with reactors treating free cyanide (Experiments A and B, see Figure 7.2), where cyanide removal percentages were greater than 90 percent for both scavenger concentrations. This decline is due to hindrance to cyanide degradation caused by the presence of copper as complexing agent. In other words the reaction,

$$\text{Cu-Cyanide} + [\bullet OH] \rightarrow \text{Products} \qquad \text{Equation 7.3}$$

is slower than the corresponding reaction of free cyanide with hydroxyl radicals,

$$CN^- + [\bullet OH] \xrightarrow{K_{CN^-,\bullet OH}=8\times10^9} \text{Products} \qquad \text{Equation 7.4}$$

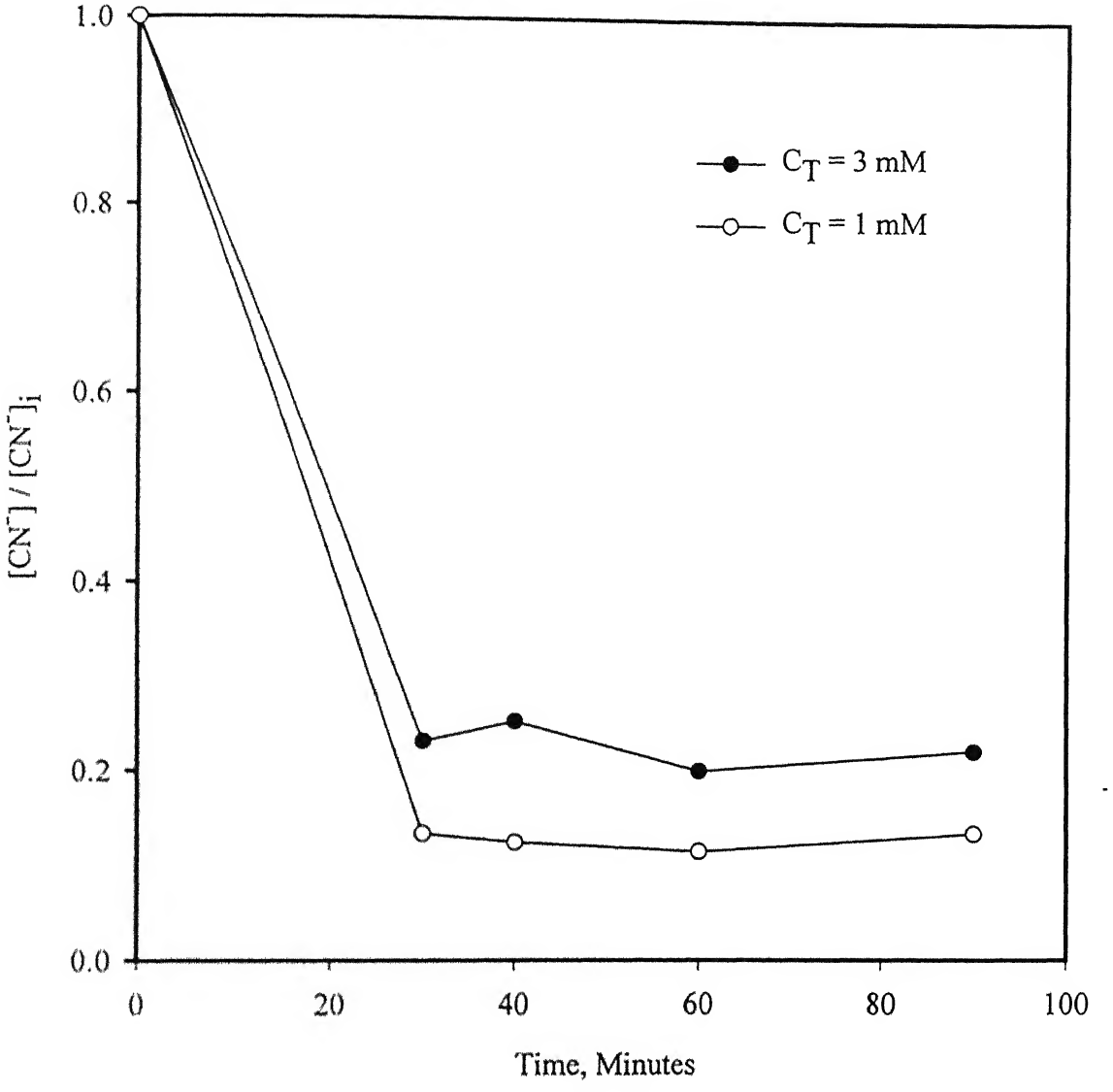

Figure 7.7 Effect of Scavenger Concentration (C_T) on Copper-Complexed Cyanide Degradation by Ozonation
($[O_3]_g$: ~37 mg/L; $[CN^-]_i$: ~ 100 mg/L; Q_g = 1.0 L/min; Q_l = 25 mL/min; V = 1 L)

The influence of liquid throughput on the copper-cyanide degradation rate by ozonation, as determined through experiments G and I are shown in Figure 7.8. The observed cyanide removal percentage at liquid throughput of 25 mL/min was 79 percent (Experiment G), as compared to 100 percent removal obtained at liquid throughput of 10 mL/min (Experiment I). These results can be explained in a similar way as in case of free cyanide (Experiments, A, D and E, see Figure 7.3).

During all three experiments concerning ozonation of copper-cyanide complexes, formation of a blue-green precipitate was observed in the reactor. This precipitate was assumed to be $Cu(OH)_2$, formed due to release of Cu(I) from copper-cyanide complexes due to ozonation. This copper was oxidized to Cu(II) and subsequently precipitated at the prevailing pH of the system. Thus for removal of copper-cyanide complexes from water during treatment operations, ozonation for the destruction of cyanide must be followed by sedimentation / filtration for the removal of the precipitated copper.

7.3.3 Evolution of By-Products

Evolution of by-products due to the ozonation of copper-complexed cyanide is presented in Figure 7.9. As in case of free cyanide (see Figures 7.4, 7.5 and 7.6), the main by-products identified and monitored were cyanate (CNO^-), ammonia (NH_3) and nitrate (NO_3^-). Cyanate (CNO^-) was determined to be the major by-product, which slowly decomposed into other products like ammonia (NH_3) and nitrate (NO_3^-). Results are also presented in Figure 7.9 in terms of nitrogen balance of the system as described earlier in case of free cyanide. Such balances were satisfactorily obtained in Experiments G and H. However for experiment I, a consistent over estimation of total nitrogen in the system was observed. The reason for this discrepancy is not immediately clear.

7.4 Discussion of Results

As discussed earlier, ozonation of free or copper complexed cyanide does not, for the main part, involve the direct reaction of molecular ozone with these species. Molecular ozone is decomposed in aqueous solution into hydroxyl [•OH] radicals, which interact

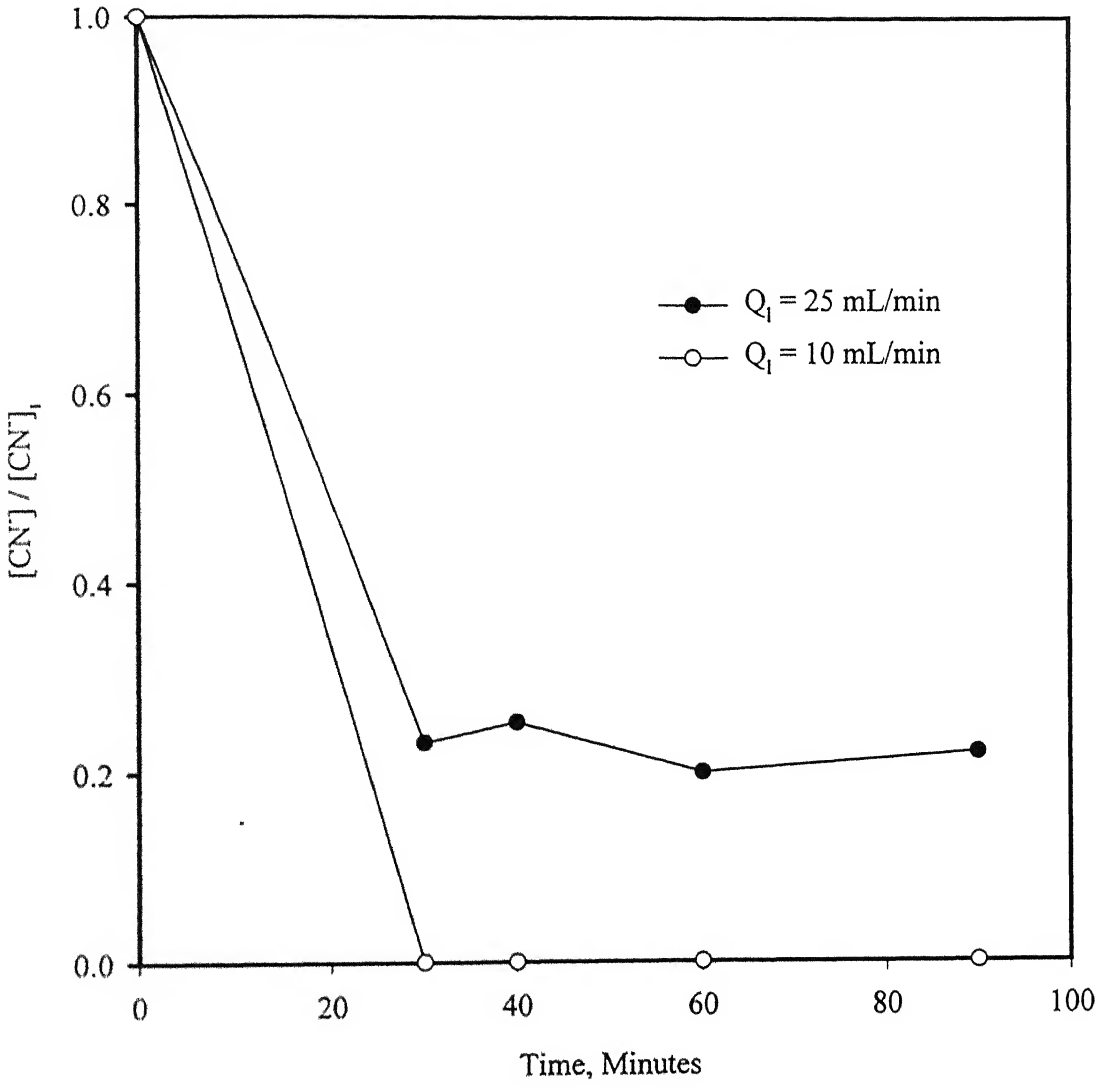

Figure 7.8 Effect of Liquid Flow Rate (Q_l) on Copper-Complexed Cyanide Degradation by Ozonation ($[O_3]_g^{\ i}$: ~37 mg/L; $[CN^-]_i$: ~ 100 mg/L; Q_g = 1.0 L/min; C_T = 3 mM; V = 1 L)

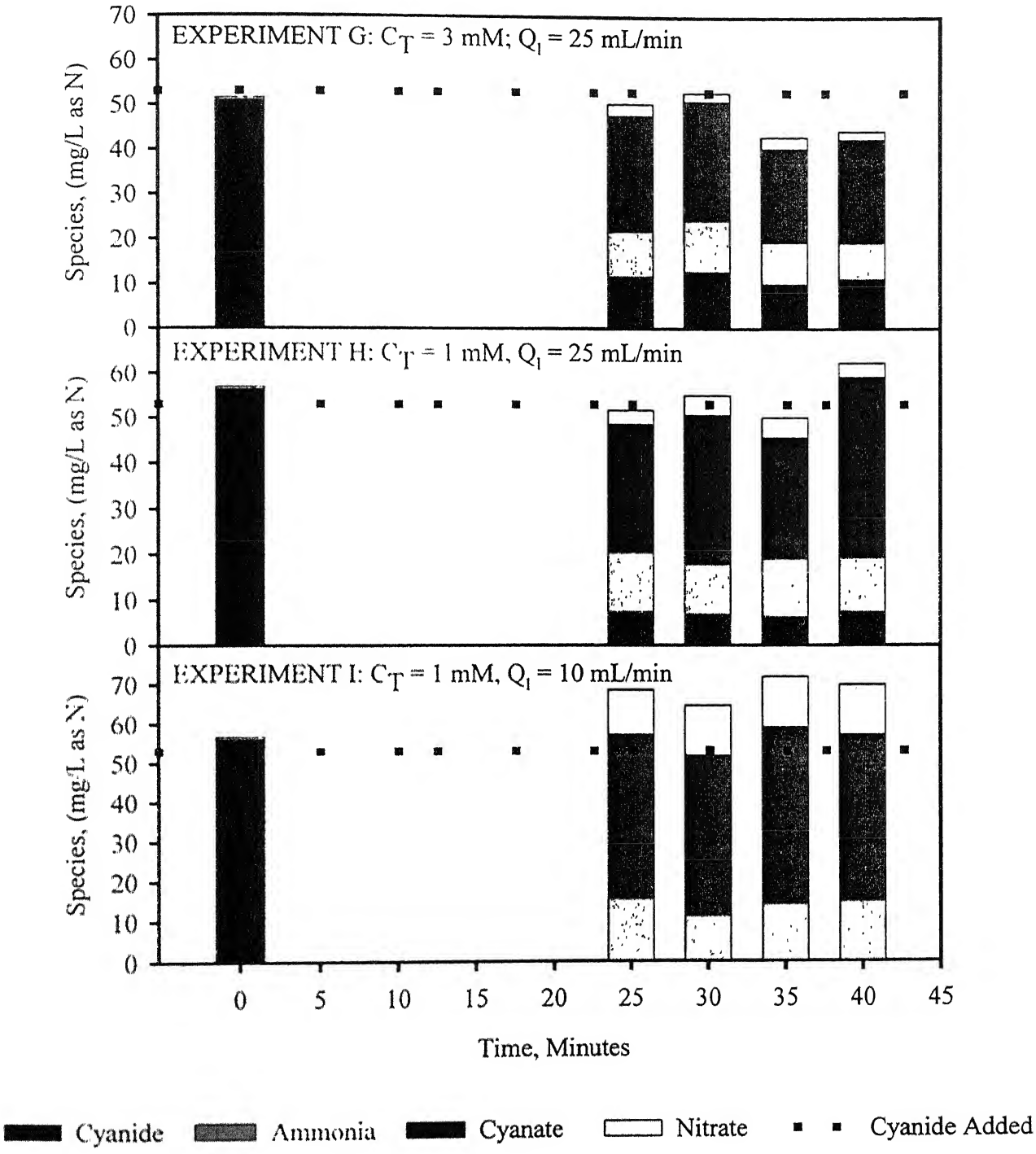

Figure 7.9 Evolution of By-Products Due to Degradation of Copper-Complexed Cyanide by Ozonation.
(Q_g = 1 L/min; V = 1 L; $[O_3]_g^{\ i}$ ~ 37 mg/L)

with cyanide and hence are responsible for cyanide degradation. As per results shown in earlier sections of this chapter, the by-products of cyanide decomposition include were cyanate (CNO^-), ammonia (NH_3) and nitrate (NO_3^-). Based on the information gathered through this research, the proposed mechanism for cyanide degradation has been presented in Figure 7.10.

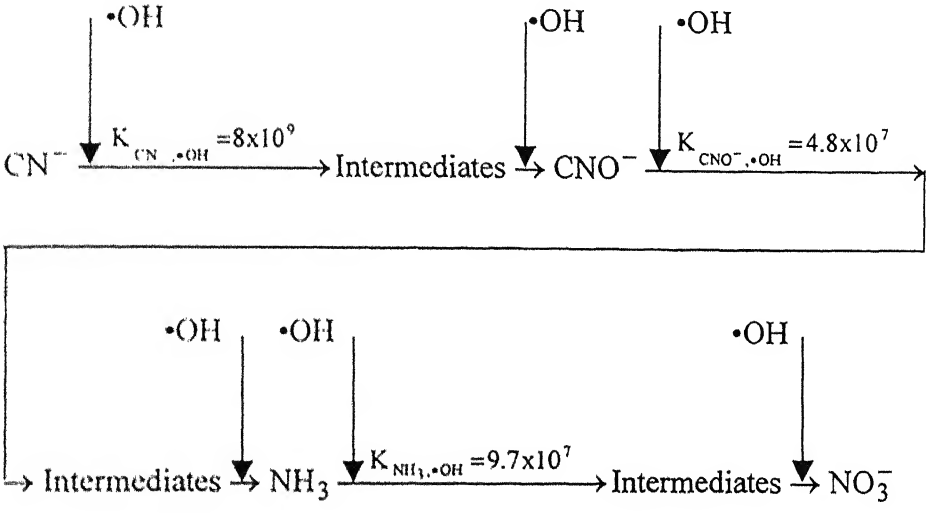

Figure 7.10 Proposed Mechanism for Cyanide Degradation and Evolution of By-Products by Ozonation at High pH

It is postulated that cyanide (CN^-) is degraded to intermediate by-products and ultimately cyanate (CNO^-) through interactions with [•OH] radicals through a relatively rapid reaction ($K_{CN^-,\bullet OH} = 8 \times 10^9$ L-mol^{-1}s^{-1}). The cyanate (CNO^-) thus formed again interacts with [•OH] radical through a slower reaction ($K_{CNO^-,\bullet OH} = 4.8 \times 10^7$ L-mol^{-1} s^{-1}) and is ultimately converted to ammonia (NH_3). The slowness of this reaction would explain the accumulation of cyanate (CNO^-) as a by-product of cyanide ozonation. Ammonia (NH_3) formed on cyanate (CNO^-) oxidation is reported to interact with hydroxyl [•OH] radicals by a relatively slow reaction ($K_{NH_3,\bullet OH} = 9.7 \times 10^7$ L-mol^{-1} s^{-1}), and is ultimately converted to nitrate (NO_3^-). This sequential reaction scheme

shown in Figure 7.10 would explain the initial appearance of cyanate (CNO^-) after start of ozonation followed by sequential appearances of ammonia (NH_3) and nitrate (NO_3^-) and later times, as shown in Figures 7.5 and 7.6.

Summary of the ozonation experiments described in this chapter is presented in Table 7.3 for free cyanide and Table 7.4 for copper-complexed cyanide. The objective of this summarization is to facilitate a discussion on the degree of ozone requirement for destruction of free and copper-complexed cyanide through ozonation. Such discussion is important for the determination of the efficiency and hence the cost of ozonation, which may then conceivably be compared to other commercial methods of cyanide degradation currently in use.

Table 7.3 Summary of Experimental Results on the Ozonation of Free Cyanide

Expt. No.	$[O_3]_g^i$, mg/L	$[O_3]_g$, mg/L	Cyanide		Rate of ozone Consumption, mg/min	Rate of Cyanide Degradation, mg/min	Stoichiometric Ratio: Ozone Consumed / Cyanide Degraded	
			Effluent, mg/L	Percent Removal			mg/ mg	mole/ mole
A	40.30±0.73	13.00	9.26	90.83	27.30	2.57	11.91	6.45
B	40.90±1.35	8.00	6.00	94.22	32.90	2.44	13.46	7.29
C	40.06±0.42	10.80	8.89	91.13	29.26	2.28	12.81	6.94
D	39.42±2.57	5.50	17.17	83.05	33.92	2.52	13.44	7.28
E	40.30±1.20	18.10	BDL*	100.00	22.20	1.10	20.12	10.90
F	35.10±0.80	8.00	18.03	83.41	27.10	2.27	11.96	6.48

* Below Detection Limit

Experiments summarized in Table 7.3 were conducted using reactor configuration and dimensions as described in Chapter IV, and under the experimental conditions as described in Table 7.1, i.e., pH 12.8; Q_g = 1 L/min; $[CN^-]_i$ ~ 100 mg/L. Results in Table 7.3 (Experiments A, B and C) indicate that greater than 90 percent removal of free

cyanide may be obtained with an influent gaseous ozone concentration ($[O_3]_g^i$) of 40 mg/L, liquid flow rate (Q_l) of 25 mL/min and scavenger concentration (C_T) of 1, 2 or 3 mM. Ozone requirement for achieving such decomposition varies between 6.45 moles (Experiment A) to 7.29 moles (Experiment B) of ozone per mole of cyanide destroyed. Cyanide removal percentages and ozone requirement were observed to be marginally higher of systems with low scavenger (C_T) concentration. This may be explained by observing that higher scavenger concentration in case of Experiment A resulted in the maintenance of lower hydroxyl [•OH] radical concentration in the reactor, which resulted in lesser cyanide removal in this reactor. At lower values of $[O_3]_g^i$, i.e., 35 mg/L, and C_T = 3 mM, cyanide removal percentage declines from above 90 percent to 83 percent (Experiment F), while ozone requirement remains nearly same (compared to Experiment A) at 6.48 moles of ozone consumed per mole of cyanide destroyed. At higher values of Q_l, i.e., 30 mL/min and C_T = 3 mM cyanide removal percentage again declines to 83 percent (Experiment D), and this decline is accompanied by an increase (compared to Experiment A) in ozone requirement to 7.28 moles per mole of cyanide destroyed. At lower values of Q_l, i.e., 10 mL/min, cyanide removal percentage increases to 100 percent (Experiment E), and this increase is accompanied by an ozone requirement (compared to Experiment A) to 10.90 moles per mole of cyanide destroyed. These results are consistent and generally in agreement with the expectation that the percentage removal of a pollutant by ozonation may be increased either by increasing the influent gaseous ozone concentration, $[O_3]_g^i$, or by lowering the liquid throughput (Q_l) through the column. Moreover, faster rate of hydroxyl [•OH] radical production in high pH systems such as the one considered here, and inherently rapid interaction between free cyanide and hydroxyl [•OH] radical ($K_{CN^-,\bullet OH} = 8 \times 10^9$ L-mol^{-1}s^{-1}) ensures that cyanide removal percentages are only marginally affected by moderate changes scavenger concentration.

The stoichiometry between ozone consumption and hydroxyl [•OH] radical production during ozonation is a complex function of reactor pH and scavenger (C_T) concentration.

However in systems with high pH, i.e., under conditions assisting ozone decomposition, this ratio is expected to be between 1 and 2. It is also known that reaction between cyanide and hydroxyl radical has a stoichiometric ratio of 1 (see Equation 7.4). Under the circumstances, requirement of six or more moles of ozone for destruction of every mole of cyanide may be explained as follows.

Hydroxyl [•OH] radical, being a very reactive, reacts with many other species present in the aqueous matrix. Under the circumstances, fraction of the generated hydroxyl radicals reacting with cyanide (CN^-), $f_{CN^-,\bullet OH}$ can be mathematically represented as,

$$f_{CN^-,\bullet OH} = \frac{K_{CN^-,\bullet OH}[CN^-]}{K_{CN^-,\bullet OH}[CN^-] + \Delta + \Lambda} \qquad \text{Equation 7.5}$$

Where,

$$\Delta = \sum k_{bi,\bullet OH}\cdot[M_{bi}] + \sum k_{si,\bullet OH}\cdot[M_{si}]$$

$$\Lambda = k_6\cdot[O_3] + k_7\cdot[H_2O_2] + k_8\cdot[HO_2^-] + k_9\cdot[\bullet HO_2] + k_{17}\cdot[HCO_3^-] + k_{18}\cdot[CO_3^{--}] + k_{19}\cdot[\bullet CO_3^-]$$

$k_{bi,\bullet OH}$ = Reaction rate constant for the i^{th} by-product of cyanide decomposition with hydroxyl radical

M_{bi} = Molar concentration of the i^{th} by-product of cyanide decomposition

$k_{si,\bullet OH}$ = Reaction rate constant for the i^{th} solute (other than those specifically accounted for) present in water with hydroxyl radical

M_{si} = Molar Concentration for the i^{th} solute (other than those specifically accounted for) present in water

A higher value of $f_{CN^-,\bullet OH}$ ensures lower stoichiometric ratio between ozone consumption and cyanide destruction. This is possible when the concentration of substances competing with cyanide for hydroxyl radical consumption is reduced. Thus better efficiency of ozone utilization vis-à-vis targeted pollutant destruction may be obtained in relatively clean waters, i.e., with low [•OH] radical consuming solute or scavenger concentration. However, it must be understood that even under the ideal

conditions, the value of $f_{CN^-,\bullet OH}$ can only increase, but never approach 1. This is due to the presence of aqueous ozone, other byproducts of ozone decomposition and by-products of cyanide degradation, all of which will interact with [•OH] radicals (see Equation 7.5) in competition with cyanide.

Experimental results summarized in Table 7.4 highlighting the salient features of experiments conducted with complexed cyanide can be explained using the similar arguments as in case of results for free cyanide summarized in Table 7.3.

Table 7.4 Summary of Experimental Results on the Ozonation of Complexed Cyanide

Expt. No.	$[O_3]_g^i$, mg/L	$[O_3]_g$, mg/L	Cyanide		Rate of ozone Consumption, mg/min	Rate of Cyanide Consumption, mg/min	Stoichiometric Ratio: Ozone Consumed / Cyanide Degraded	
			Effluent, mg/L	Percent Removal			mg / mg	mole / mole
G	39.56±1.65	7.80	21.00	74.00	31.76	1.85	17.17	9.30
H	39.56±1.82	3.30	14.00	91.00	36.26	2.28	15.94	8.63
I	39.44±1.44	14.90	BDL*	100.00	24.54	1.05	23.37	12.66

* Below Detection Limit

Comparison of Experiments G and H show that cyanide removal percentage is lower for experiment G as compared to experiment H. Here it may be pointed out that these two experiments are similar in all respects except for scavenger concentration (C_T) which is 3 mM and 1 mM for Experiment G and H respectively. Hence, it may be concluded that as in case of experiments with free cyanide, higher scavenger concentration in case of Experiment G resulted in the maintenance of lower hydroxyl [•OH] radical concentration in the reactor, thus resulting in lesser cyanide removal.

Comparison of Experiment G with the corresponding experiment with free cyanide (Experiment A, summarized in Table 7.3) indicate that cyanide removal percentage was lower in case of Experiment G. This may be due to the lower rate of interaction between

complexed cyanide and hydroxyl [•OH] radicals, as compared to similar interactions with free cyanide. Similar comparison between Experiment H with the corresponding experiment with free cyanide (Experiment B, summarized in Table 7.3) indicate that cyanide removal percentage was marginally lower in case of Experiment H also. It is also noticed that stoichiometric ozone requirement of cyanide destruction was higher in case of experiments with complexed cyanide, probably due to additional hydroxyl [•OH] radical consumption by Cu (I), released during decomposition of copper-cyanide complexes, in competition with free cyanide.

REFERENCES

APHA, AWWA, WPCF. (1995). Standard Method for Examination of Water and Wastewater. 19th Edition, APHA, Washington D.C.

APHA, AWWA, WPCF. (1985). Standard Method for Examination of Water and Wastewater. 16th Edition, APHA, Washington D.C.

Anselmi, G., Lignola, P. G., Raitano, C., and Volpicelli, G. (1984). "Ozone Mass Transfer in Stirred Vessel". Vol. 6, p17.

Bader, H. and Hoigne, J. 1981. "Determination of Ozone in Water by Indigo Method." Wat. Res. Vol. 15. p449.

Bailey, P.S. 1972. "Organic Groupings Reactive Towards Ozone-Mechanisms in Aqueous Media." Ozone in Water and Wastewater Treatment, (Evans, F.L. Editor), Ann Arbor Sci. Publ., Inc., Ann Arbor MI.

Bailey, P.S. 1978. "Ozonation in Organic Chemistry." vol. I-Olefinic Compounds. (Trahanovsky, W. Editor), Academic Press, New York NY.

Balden, A. R. (1959). "Treatment of Industrial Process wastes at Crystler Corporation". Sewage and Industrial Wastes. Vol. 31, p394.

Beltran, F. J., Garcia-Araya, J. F. and Encinar, J. M. (1997). "Henry and Mass Transfer Coefficients in Ozonation of Wastewater". Ozone Sci. and Engrg., Vol. 19, p281.

Benefield, L. D., Judkins, F. J. and Weand, B. L. (1982). Process Chemistry for Water and Wastewater Treatment. Prentice-Hall Inc. Englewood Cliffs, New Jersy, USA.

Benitez, F. J, Acero, J. L., Gonzalez, T. and Garcia, J. (2001). "Ozonation and Biodegradation Processes in Batch Reactors Treating Black Table Olives Washing Wastewaters". Ind. Eng. Chem. Res., Vol. 40, p3144.

Bin, A. K. (1995). "Application of Single Bubble Model in Estimation of Ozone Transfer Efficiency in Water". Ozone Sci. and Engrg. Vol. 17, p469.

Capiro, V., Insola, A., Lignola, P. G., and Volpicelli, G. (1981). "A New Attempt for the Evaluation of Absorption Constant of Ozone in Water". Chemical Engrg, Vol. 37, p122.

Cogo, E., Albet, J., Malmary, G., Coste, C. and Molinier, J. (1999). "Effect of Reaction Medium on Ozone Mass Transfer Applications to Pulp Bleaching". Chemical Engrg J., Vol. 73, p23.

Dobson (1947). "The Treatment of Cyanide Wastes by Chlorination". Sewage Works Journal, Vol. 19, p1007.

Dore, M. 1985. "Different Mechanisms of the Action of Ozone on Aqueous Organic Micropollutants." Proc. Intl. Conf. The Role of Ozone in Water and Wastewater Treatment. London. ed. Perry, R. and McIntyre, A.E. 13-14 Nov. 1985.

Edwards, G.A., and Amirtharajah, A. 1985. "Removing Color Caused by Humic Acid." Journal. Am. Wat. Wrks. Assn. Vol. 77. No. 3. p50.

Filbeck, W. J. and Mattock, G. (1987). Chemical Processes in Wastewater Treatment. Ellis Horwood Limited.

EPA Capsule Report (2000). Managing Cyanide in Metal Finishing. EPA 625/R-99/009. National Risk Management Research Laboratory, Technology Transfer and Support Division, Cincinnati, Ohio.

Frant, M. S., Ross, J. W. and Riseman, J. H. (1972). "Electrode Indicator Techniques for Low Levels of Cyanide". Analytical Chemistry, Vol. 44, p2227.

Garrett, R. L., Garland, R. C. and Sawyer Jr., T. (1958). "How Transworld Airlines Treats Plating Shop Wastes". Plating, Vol., 45, p847.

Glaze, W.H., Kang, W.H. and Chapin, D.H. 1987. "The Chemistry of Water Treatment Processes Involving Ozone, Hydrogen Peroxide and Ultraviolet Radiation." Ozone Sci.and Engg. Vol. 9. No. 4. p335.

Gonsalves, M. M. M. A. F. Pinto, A. F. and Granato, M. (1998). "Biodegradation of Free Cyanide, Thiocyanate and Metal Complexed Cyanides in Solutions with Different Compositions." Environmental Technology, Vol. 19, No. 2, p133.

Gurnham, C. F. (1944). "Cyanide Destruction on Trickling Filters". Proc. 10th Ind. Waste Conf., Purdue University, p186.

Gurol, M. D., Bremen, W. M. and Holden, T. E. (1985). "Oxidation of Cyanide in Industrial Wastewater by Ozone". Environmental Progress, Vol. 4, p46.

Hartinger, L. (1994). Handbook of Effluent Treatment and Recycling for Metal Finishing Industry. 2nd Edition. Finishing Publications.

Hoigne, J. and Bader, H. 1976. "The Role of Hydroxyl Radical Reactions in Ozonation Processes in Aqueous Solutions." Wat. Res. Vol. 10. p377.

Hoigne, J. and Bader, H. 1979. "Ozonation of Water: 'Oxidation-Competition Values' of Different Types of Water Used in Switzerland." Ozone Sci. and Engg. Vol. 1. No. 4., p357.

Hoigne, J. and Bader, H. 1983a. "Rate Constants of Reactions of Ozone with Organic and Inorganic Compounds in Water-II. Non-Dissociating Organic Compounds." Water Res. Vol. 17 p173.

Hoigne, J. and Bader, H. 1983b. "Rate Constants of Reaction of Ozone with Organic and Inorganic Compounds in Water-I. Dissociating Organic Compounds." Water Res. Vol. 17. p185.

Hoigne, J., Bader, H., Haag, W.R. and Staehelin, J. 1985. "Rate Constants of Reactions of Ozone with Organic and Inorganic Compounds in Water-III. Inorganic Compounds and Radicals." Water Res. Vol. 18. No. 8. p993.

INCO (1993). Cyanide Destruction: The INCO SO_2/Air Process. Inco Exploration and Technical Services.

Katzenelson, E.B. and Shuval, H.I. 1974. "Inactivation Kinetics of Viruses and Bacteria in Water by Use of Ozone." Journal Am. Wtr. Wrks. Assn. Vol. 66. p725.

Kandelwal, K. K., Barduhn, A. J., and Grove Jr., C. S. (1959). "Kinetics of Ozonation of Cyanides". Advances in Chemistry Series No. 21, ACS, p78.

Langlais, B., Reckhow, D.A. and Brink, D.R. Editors. 1991. Ozonation in Water Treatment. Aplications and Engineering. Cooperative Research Report. AWWRF and Compagnie Generale des Eaux. Lewis Publishers.

Laplanche, A., Le Sauze, N., Martin, G. and Langlais, B. (1991). "Simulation of Ozone Transfer in Water: Comparison with a Pilot Unit". Ozone Sci. and Engrg. Vol. 34, p535.

Lee, B. N and Lou, J. C. (2000). "Study on wet air oxidation of aqueous ferrous cyanide solution catalyzed by three metal salts". Water Science & Technology, Vol. 42, No 3-4, p131.

Matsuda, Y., Fujisawa, T., Fujikawa, S., Takasu, Y., Tanaka, Y. and Imagawa, H. (1975). "Oxidation of Cyanide Ion in Aqueous Alkaline Solution by Ozone". J. Chem. Soc. Japan, Vol. 4, p602.

Masschelein, W. J. (1982). Contacting Ozone with Waterand Contactor Offgas Treatment. In: Handbook of Ozone Technology and Applications. Ed: Rip G. Rice and A. Netzer. Ann Arbor Science Publishers, Ann Arbor, Michigan.

Mendes, P. (1993). GEPASI: a software package for modeling the dynamics, steady states and control of biochemical and other systems. *Comput. Appl. Biosci.* 9, pp563-571.

NDRL. (2002). Notre Dame Radiation Laboratory, Radiation Chemistry Data Centre. Web Address: http:// allen.rad.nd.edu/

Nishikawa, M., Nakamura, M., Yagi, H., and Hashimoto, K. (1981). "Gas Absorption in Aerated Mixing Vessels". J. Chemical Engrg. Of Japan, Vol. 14, p214.

O'Donovan, D.C. 1965. "Treatment with Ozone." Journal Amer. Wtr. Wrks. Assn. Vol. 9. p1167.

Pablo, F., Stauber, J.L., Buckney, R.T. (1997). Toxicity of Cyanide and Cyanide Complexes to the Marine diatom Nitzchia closterium. Water Research, Vol. 31, p2435.

Patterson, J. W. (1985). Industrial Wastewater Treatment Technology. Second Edition, Butterworths Publication, Stoneham, USA.

Peleg, M. 1976. "Review Paper-The Chemistry of Ozone in the Treatment of Water." Water Res. Vol. 10. p361.

Rice, R.G., Robson, C.M., Miller, G.W. and Hill, A.G. 1981."Uses of Ozone in Drinking Water Treatment."Journal Am. Wtr. Wrks. Assn. Vol. 73 p44.

Roth, J.A. and Sullivan, D.E. 1983. "Kinetics of Ozone Decomposition in Water." Ozone Sci. and Engg. Vol. 5. No. 1. p37.

Roustan, M., Duget, J. P., Brette, B., Brodard, E., and Mallevialle, J. (1987). "Mass Balance Analysis of Ozone in Conventional Bubble Contactors". Ozone Sci. and Engrg. Vol. 9, p289.

Rowley, W. J., Otto, F. D. (1980). "Ozonation of Cyanide with Emphasis on Gold Mill Wastewaters". Can. J. Chem. Eng. Vol. 58, p646.

Sax, N. I., and Lewis, R. J. (1989). Dangerous Properties of Industrial Materials. 7th Edition. Van Nostrand Reinhold, New York, New York.

Selm, R. P. (1959). "Oxone Oxidation of Aqueous Cyanide Waste Solutions in Stirred Batch Reactors and Packed Towers". Advances in Chemistry Series No. 21, ACS p66.

Sondak, N. E., and Dodge, B. F. (1961). "The Oxidation of Cyanide Bearing Plating Wastes by Ozone". Part I, Plating, Vol. 48, p180.

Sontheimer, H., Heilker, E., Jekel, M.R.,Nolte, H. and Vollmer, F.H. 1978. "The Mulheim Process." Journal Am. Wtr. Wrks. Assn. Vol. 70. No. 7. p393.

Sontheimer, H. 1985. "ROUNDTABLE. Trends in Ozonation." Journal Am. Wtr. Wrks. Assn., Vol. 77. p19.

Sotelo, J. L., Beltran, F. J., Gonzalez, M. and Dominguez, J. (1989). "Effect of High Salt Concentrations on Ozone Decomposition in Water". J. Envir. Sci. Health., Vol. A24, p823.

Staehelin, J.H. and Hoigne, J. 1982. "Decomposition of Ozone in Water: Rate of Initiation by Hydroxide Ions and Hydrogen Peroxide." Environm. Sci. and Tech.,Vol. 16. No. 10. p676.

Staehelin, J.H. and Hoigne, J. 1985. "Decomposition of Ozone in Water in the Presence of Organic Solutes Acting as Promoters and Inhibitors of Radical Chain Reactions." Environm. Sci. and Tech. Vol 19. p120.

Streebin, L.E., Schornick, H.M., Wachinski, A.M. (1981). "Ozone Oxidation of Concentrated Cyanide Wastewater from Electroplating Operations", p665, Proceedings of 35th Purdue Industrial Waste Conference, Indiana.

Szpyrkowicz, L., Zilio-Grandi, F., Kaul, S. N., and Rigoni-Stern, S. (1998). "Electrochemical treatment of copper cyanide wastewaters using stainless steel electrodes". Water Science and Technology, Vol 38, No 6, p261.

Travin, D. (1956). "Metal Plating Wastes and Sewage Treatment". Sewage and Industrial Wastes, Vol. 28, p1371.

Trussel, R.R. and Umphres, M.D. 1978. "The Formation of Trihalomethanes." J. Am. Wtr. Wrks. Assn. Vol. 70, p604.

Tyler R.G., Maske, W., Matthew, W., and Westin, M.J. (1949). "The Ozonation of Cyanide Wastes". Proceedings of 6th Purdue Industrial Wastewater Conference, Indiana

Walker, C. A. and Zabban, W. (1953). "Disposal of Plating Room Wastes, IV. Treatment of Plating Room Waste Solutions with Ozone". Plating, Vol. 40, p777.

Wise, W. S. (1948). "The Industrial Waste Problem. IV. Brass and Copper, Electroplating and Textile Wastes. Sewage Works Journal, Vol. 20, p96.

Wu, J. J. and Masten, S. J. (2001). "Mass Transfer of Ozone in Semibatch Stirred Reactor". Journal of Environmental Engineering, Vol. 127, p1089.

Yurteri, C. 1988. "Removal of Organic Pollutants by Ozonation: Kinetics and Reactor Design." Ph.D. Dissertation, Drexel University.

Zeelvalkink, J. A., Visser, D. C., Arnoldy, P. and Boelhouwer, C. (1979). "Mechanism and Kinetics of Cyanide Ozonation in Water". Water, Res. Vol., 14, p1375.

Zhou, H. and Smith, D. W. (2000). "Ozone Mass Transfer in Water and Wastewater Treatment: Experimental Observations Using 2D Laser Particle Dynamics Analyzer"." Water Research, Vol. 34, p909.